TradeRES

New Markets Design & Models for 100% Renewable Power Systems

New forecast tools to enhance the value of VRE on the electricity markets

Deliverable number:	*D4.9*
Work Package:	*WP4*
Lead Beneficiary:	*LNEG*

This project has received funding from the European Union's Horizon 2020 research and innovation programme under grant agreement No 864276

Author(s) information (alphabetical)		
Name	**Organisation**	**Email**
Ana Estanqueiro	LNEG	ana.estanqueiro@lneg.pt
António Couto	LNEG	antonio.couto@lneg.pt
Christoph Schimeczek	DLR	christoph.schimeczek@dlr.de
Duarte Lopes	Enlitia	duarte.lopes@enlitia.com
Hugo Algarvio	LNEG	hugo.algarvio@lneg.pt
Isabel Preto	Enlitia	isabel.preto@enlitia.com
Johannes Kochems	DLR	johannes.kochems@dlr.de
Tiago Santos	Enlitia	tiago.santos@enlitia.com
Ricardo Faria	Enlitia	ricardo,faria@enlitia.com
Evelyn Sperber	DLR	evelyn.sperber@dlr.de

Document information			
Edition	**Date**	**Dissemination Level**	**Description**
1	25.10.2021	Public	In this report the implementation of new forecasting techniques and time synergies is explained.
2	**26.01.2024**	**Public**	**This edition improves the forecasting techniques presented in the first edition and presents models to be used in the short-term forecasts.**

Review and approval		
Prepared by	**Reviewed by**	**Approved by**
See list above	Débora de São José, Fernando Lezama (ISEP)	Ana Estanqueiro

Disclaimer

Executive Summary

The present deliverable was developed as part of the research activities of the TradeRES project *Task 4.4 - Enhancing the value of VRE on the electricity markets with advanced forecasting and ramping tools* edition 2.

This report presents the second edition of deliverable 4.9, which consists of the description and implementation of the forecasting models aiming to identify and explore the time synergies of meteorological effects and electricity market designs explored in the project to maximize the value of variable renewable energy systems and minimize market imbalances.

An overview of key aspects that characterize a power forecast system is presented in this deliverable through a literature review. This overview addresses the: i) forecast time horizon; ii) type of approach (physical, statistical or hybrid); iii) data pre-processing procedures; iv) type of forecast output; and v) the most common metrics used to evaluate the performance of the forecast systems.

While in the TradeRES project work package 3 the conception of new market designs and products are presented from a theoretical point of view, in this deliverable, the power forecast tools capable to address the new designs and products are presented and discussed. Complementarily to the first edition of this deliverable, the link between day-ahead market time frames and the performance of the different power forecast approaches is analysed. This second edition of D4.9 also focuses on the short-term forecasts (below six hours) for new market designs.

As a first step, a non-disruptive change in the day-ahead market is proposed by simply postponing the gate closure hour according to the meteorological data availability from the global numerical weather prediction (NWP) models while the 24 hours forecast periods are still used. In the second step, various short-term forecast approaches designed for time horizons below six hours are developed and implemented. These approaches are specifically tailored to attend the requirements of new electricity market designs currently under development in TradeRES.

Another aspect regarding the meteorological time synergy and electricity markets analysed in this deliverable is the identification of extreme events. A wind power ramping forecast approach implemented in the TradeRES forecast tools is described. This approach is designed to complement the existing deterministic power forecasts and it can be used to increase the transmission system operators' awareness level and helping them to better scale the level of reserve required. Market players can also take advantage of this information to strategically define the bids in the different market environments.

Using different wind and solar power parks in Portugal, as well as the national aggregated Portuguese and German wind and solar generation, results regarding the potential certainty gain effect from changing the day-ahead market gate closure are presented and analysed in this deliverable. Results showed that the use of the TradeRES forecast methodology guaranteed better performance compared to an operational forecast from a forecast provider. Additionally, the results emphasized the benefits of including non-traditional variables such as air pressure and temperature at different heights, atmospheric boundary

layer, and geopotential height for various pressure levels. The simulations also highlighted that incorporating both NWP features based on historical power series led to improvement when compared with models based solely on power series or NWP. Therefore, it is recommended that power forecast systems can have access to recent observed values to improve their accuracy.

Despite the improvements achieved in the forecasts for the day-ahead market, high power forecast errors are still observed (a normalised root mean square error of nearly 30% for wind and solar in Portugal and nearly 20% for Spain). Market designs with shorter forecast time horizons can significantly reduce power forecast errors. Results also emphasize the importance of evaluating the most suitable forecast approach based on the forecast time horizon. To assess the value of renewable energy forecasting for the German day-ahead market, the Agent-based Market model for the Investigation of Renewable and Integrated energy Systems (AMIRIS) was enhanced to account for power forecast errors. For this purpose, a feature was developed that allows for the adjustment of forecasts for the feed-in of renewable energies using a Gaussian distributed error term. Furthermore, this deliverable presents a realistic forecast time series that was implemented in AMIRIS. The case study of the German day-ahead market in 2019 demonstrated that realistic power forecasts can reduce the profits of onshore wind turbine operators by approximately 8% compared to perfect foresight of wind infeed. Assuming Gauss-distributed errors, the losses are smaller (~ 5 % less profit compared to the perfect forecast).

The power forecast tools developed in this task will be publicly shared and disseminated in the channels of the project. With this step, users can use the tools for obtaining power forecasts in future studies or use the approaches developed in TradeRES as a benchmark.

Table of Contents

List of Tables

List of Figures

List of Abbreviations

AMIRIS	Agent-based Market model for the Investigation of Renewable and Integrated energy Systems
ANN	Artificial neural networks
AR	Autoregressive
ARIMA	Autoregressive integrated moving average
ARMA	Autoregressive Moving Average
Bias	Bias Score
BRPs	Balance responsible parties
CFD	Computational fluid dynamics
DAM	Day-Ahead Market
ECMWF	European Centre for Medium-Range Weather Forecasts
FN	False negative
FP	False positive
GFS	Global Forecast System
hPa	Hectopascal
IBC	Initial and Boundary Conditions
IDM	Intraday markets
KNN	K-nearest neighbour
KSS	Hanssen & Kuipers Skill Score
Lat	Latitude
Long	Longitude
MA	Moving Average
MAPE	Mean absolute percentage error
MATREM	Multi-Agent TRading in Electricity Markets
Meso	Mesoscale numerical model
Micro	Microscale numerical model
ML	Machine Learning
MLWP	Machine Learning-based weather prediction model
NB	Normalized bias
NRMSE	Normalized root mean square error
NWP	Numerical Weather Prediction
OF	Objective function
PAM	Period ahead market
PCA	Principal component analysis
PCs	Principal components
PDF	Probability density functions
POD	Probability of detection
PV	Photovoltaic
RF	Random Forest
RMSE	Root mean square error
NRMSE	Normalized RMSE
SCADA	Supervisory control and data acquisition
SFF	Sequential forward feature
SIDC	Single Intraday Coupling
SVM	Support vector machine
TCT	Target-circulation types
TN	True negative
TP	True positive
TSO	Transmission System Operator
UTC	Universal time coordinated
vRES	variable Renewable Energy Sources
WP	Work package
WR	Weather regime
WRF	Weather Research and Forecasting
XAI	Explainable artificial intelligence

1. Introduction

The present deliverable was developed as part of the research activities of the TradeRES project's *Task 4.4 - Enhancing the value of VRE on the electricity markets with advanced forecasting and ramping tools* (work package 4). This report presents the second edition of deliverable D4.9 which consists of the description of forecasting techniques implementation aiming to identify and explore the time synergies of meteorological effects and electricity market designs to maximize the value of variable renewable energy systems and minimize market imbalances. The initial edition of D4.9 concentrated on understanding the forecasting approaches available and proposed a new forecast approach for existing market designs. This second edition presents the results of approaches proposed applied to various case studies (at national and power plant levels) and it addresses new forecast approaches tailored to new market designs introduced in the project focusing on trading with a shorter lead time horizon (up to six hours).

One of the most important challenges in the energy sector is the large-scale integration of renewable energy sources (particularly, variable renewable energy sources - vRES such as wind and solar) into electrical power systems in an economic and environmentally sustainable way. Transmission system operators (TSOs) must always ensure the balance between electricity production and consumption. Currently, a safe and robust operation of a power system needs highly accurate forecasts of both vRES power production and consumption to minimize the need for balancing the energy in the reserve markets, typically at high costs [1]–[3]. With near to 100% renewable power systems, the role of the forecast system and its accuracy will be even more relevant.

Forecasts are also important to electricity markets. To participate in the different products from electricity markets, market players/actors need to rely on forecast systems to build their bids. With the existing market designs, when power producers do not follow the scheduled bid, they are penalized and their profits are strongly decreased [4]. Due to the intrinsic chaotic nature of atmosphere, the participation of vRES players in the existing markets is still a challenge, especially, when long time horizon forecasts are needed. In work package (WP) 3 of TradeRES project the shortcomings and alternative designs for a near 100% renewable electricity system were addressed. For day-ahead market (DAM), which is the most used and with highest liquidity market, the authors of deliverable 3.5 [5] suggested a reduction of the time gap between the DAM closure hour and the forecast's delivery time while keeping the current organization of wholesale electricity trade. Nevertheless, it is necessary to assess if the new gate closure's timing are enough to reduce expressively the vRES power forecast errors, or if it is necessary to replace the existing designs [5]. Therefore, to design electricity markets that are adequate to vRES trading it is crucial to understand the capabilities of power forecast systems as well as how they work in order to i) identify potential new time frames for this specific market, ii) identify the players that have more challenges to participate in the existing DAM, and iii) develop the forecast tools required for TradeRES project and the electricity markets for 2030 and beyond.

According to the second edition of D3.5 from TradeRES project [6], an alternative to current market designs *"is a shift towards more frequent trading, e.g., clearing the market*

every hour for delivery six hours later". This shift requires the adoption of new forecast models (*e.g.*, autoregressive models) for vRES power. According to several authors, for this timeframe, these models typically surpass the performance of the NWP. Consequently, different forecast methods tailored to this new timeframe are proposed and analysed for different case studies.

Another aspect regarding the synergy between meteorological timings and electricity markets refers to the identification of extreme events. Extreme events as wind power ramps usually have a significant impact on the electricity markets [7], [8]. In the case of wind power ramps, the early identification and forecasting of these events triggered by weather conditions can allow to raise the level of Transmission system operators' (TSOs) awareness helping them to better scale the level of risk that exists for the power system [8] as well as commit additional reserves, to minimize operational risks. This information is designed to complement traditional time-series forecasts rather than replace them, enabling, for instance, the dynamic allocation of necessary reserves. Market players can also take advantage of this information to participate strategically in electricity markets since, under these conditions, large vRES forecast errors in DAM are expected [8].

Forecast of wind power ramps is a relatively novel research topic and the works already published highlight that the trigger mechanisms of such events are rarely similar across the control regions or wind parks [9]. Nevertheless, one of the most successful approaches to understand and forecast the dynamics of wind power ramps involves the use of holistic approaches capable of accounting the spatial and temporal development of atmospheric large-scale circulation [8], [10]. In [8], an automated cyclone detection algorithm was implemented to identify challenging weather situations for the TSO. In [10], the authors also applied an automated cyclone detection algorithm and compared its performance with a windstorm algorithm. The highest performance to detect wind power ramps is observed with the windstorm detection algorithm. Nevertheless, all the previous algorithms have a common shortcoming: a wind power ramp is neither always a consequence nor it is always linked to the existence of extreme wind speed values, being essentially dependent from the previous (historical) state of the atmosphere. In this sense, a new algorithm that uses a time numerical differentiation to fit the particular case of wind power ramps events was developed and is presented in this deliverable.

This deliverable is organized as follows: an overview regarding the power forecast systems is provided in section 2. In section 3, the link between electricity market periods and power forecast errors and source of information is discussed. Section 4 provides a contextualization and description of various forecast approaches developed in the project. Section 5 presents results using national wind and solar power data from Portugal, Spain, and Germany, along with data from several wind and solar power plants in Portugal. Section 6 briefly presents some final remarks.

2. Power forecasts

The forecasting problem is transversal to several sectors of activity, such as financial, scientific, industrial, political, etc. In the energy sector, several systems have been developed in the recent years to predict the power output from wind or solar power plants as well as the electricity demand. Typically, forecast is conducted at a specific time, *t*, for a future time horizon, *t+k.* Despite advancements in forecast tools and approaches, the energy sector in European countries predominantly focuses on predicting the average power, P_{t+k}, expected to be provided to the grid at time *t+k*. In the literature, several classifications for the power forecast systems are available [11]. These systems can be classified according to the forecast time horizon and type of approach. In the next subsections, these classifications are addressed as well as some of the additional steps to implement a forecast system.

It should be noted that this chapter provides a summary of approaches commonly applied in the energy sector aiming to highlight the different options available. This background is important to establish how to proceed to implement the forecast approaches most suitable to the different needs of the project. Comprehensive reviews are available for wind [1], [2], [11], [12] and solar photovoltaic (PV) [13]–[15] power forecasting.

2.1 The forecasting process and objectives

The forecasting process aims to transform one or more independent variables (inputs) into one or more dependent variables (outputs). This process is characterized by some key steps [16]:

- Problem definition
- Data collection
- Descriptive data analysis
- Forecast model selection
- Model validation
- Forecast
- Performance evaluation

Problem definition consists of evaluating the forecast period, forecast horizons and the time step of the outputs. The type of output needed and the establishment of admissible errors in the results are also established in this step. In the data collection phase, the variables under study (object of the forecast) and the independent variables necessary to build the forecast model need to be collected. For the descriptive analysis of the data, it is necessary, in the first place and when working with a time series, to take into account that successive observations are not independent events [17], and as such, the order of observations must be respected. According to [16], to obtain greater sensitivity of the data under analysis, they should be represented in the form of a temporal graph and a summary of some statistical parameters should be computed. This procedure makes possible to identify anomalies in the data, trends and seasonality that otherwise might not be evident.

After analysing the data, the forecasting method is applied. This task consists of choosing and adjusting one or more models to the specific case study, that is, reproducing the dependent variable, depending on the independent variable (or variables), within a certain margin of error. The model selection should take into consideration aspects as the time horizon and the type of information expected from these models (deterministic, probabilistic, or ramp event forecast). Once selected, the method must be validated. This validation is done by assessing the performance of the forecast. For this purpose, the method is normally adjusted to only a part of the available data, with the rest being used for its validation. Once validated, the method is implemented and its control is carried out continuously by measuring the forecast errors (e.g., bias) to verify the continued validity of the method, and, if necessary, make all necessary updates to reduce the errors.

2.2 Forecast time horizon

The time duration for which the power output is forecast is known as the forecast time horizon. The forecast horizon of interest depends on the different applications, and in energy sector it can be divided into four main time scales: very short-term, short-term, medium-term, and long-term [1], [18], [19]. The time frames of this classification can slightly change among the different authors. The application for the different time frames is depicted in Table 1.

Table 1. Time horizon, temporal scale and common application of the forecast approaches [20].

Time horizon	Temporal scale	Applications
Very short	From seconds to 30 minutes	- Real-time dispatch and regulation operations on the network; - Forecasting the consumption of buildings in the context of micro-grids; - Coordinating real-time demand response programs.
Short	From 30 minutes to 6 hours	- Impacts on energy price determination in intraday markets; - Support decisions on the status of network loads; - Support the decision to turn-on or off the generator set with quick response; - Security operations for the energy market.
Medium	Varies between 6 hours and 1 day	- Support the decision to turn generators on or off; - Safety time horizon for the day-ahead market; - Impacts on energy price determination; - Allocation of power reserves.
Long	More than a day	- Planning of maintenance operations; - Power system adequacy planning; - Strategic capacity planning.

2.3 Type of approach

In this section, the most common types of forecast approaches used in the energy sector are presented. Figure 1 illustrates the recommended sources of information and forecast approaches based on their spatial and temporal horizons that will be further analysed in the next subsections.

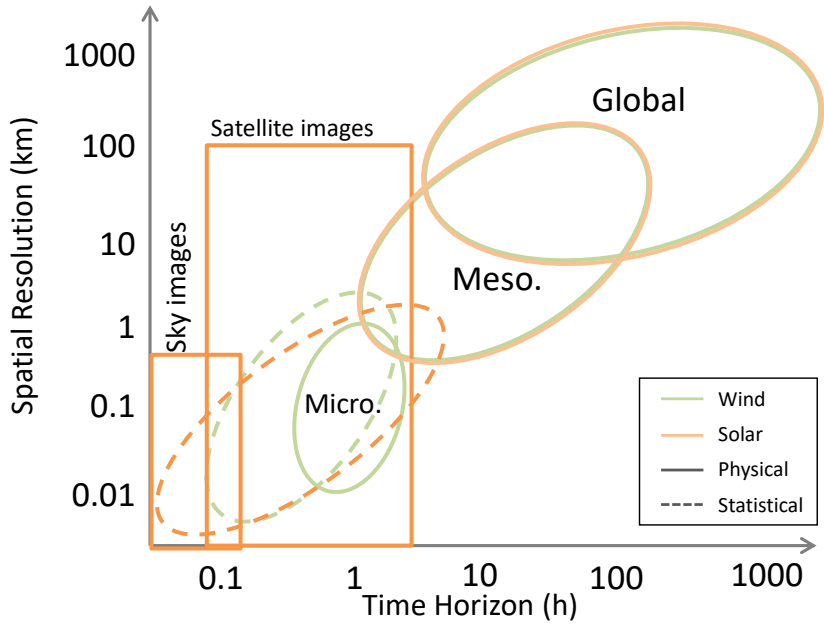

Figure 1. Recommended source of information/approach for solar and wind for the different time horizons and spatial resolution. Adapted from [21].

2.3.1. Physical approaches

The physical power forecast approaches are mainly based on the use of numerical meteorological models – Numerical Weather Prediction (NWP), which parameterize and simulate in detail the atmosphere and its circulation mechanisms. NWP models provide meteorological parameters as wind components, cloud coverage, air temperature, and pressure, that are used to generate forecasts.

This type of model is being developed since 1950 when NWP models were used to make weather forecasts with time horizons on the scale of days. They were, however, very primitive models based on quasi-geostrophic theories where it was impossible, either due to lack of knowledge or lack of computational resources, to include relevant physical processes (radiation processes and phase transition) to make reliable predictions [22]. Over the years and with substantial technological improvement, these models and the parameterizations that govern them were improved and the relevant physical processes missing were progressively added. Currently, these models are still the core of weather forecasting and have evolved substantially following the growing knowledge regarding the physical processes that govern the atmosphere dynamics and its circulation as well as the computational capabilities.

NWP models are, nowadays, less simplistic and with more detailed and precise physical parameterizations. Additionally, these models benefited from more efficient and representative data acquisition and assimilation systems around the globe, which include meteorological stations, satellite data, radiosondes and measurements performed by airplanes and ships. All these improvements have led to a significant decrease in the forecast errors in the recent years, as reported for the operational European Centre for Medium-Range Weather Forecasts (ECMWF) model, Figure 2. This figure also highlights that

the errors are significantly higher for a time horizon of five-days compared to one-day time-horizon.

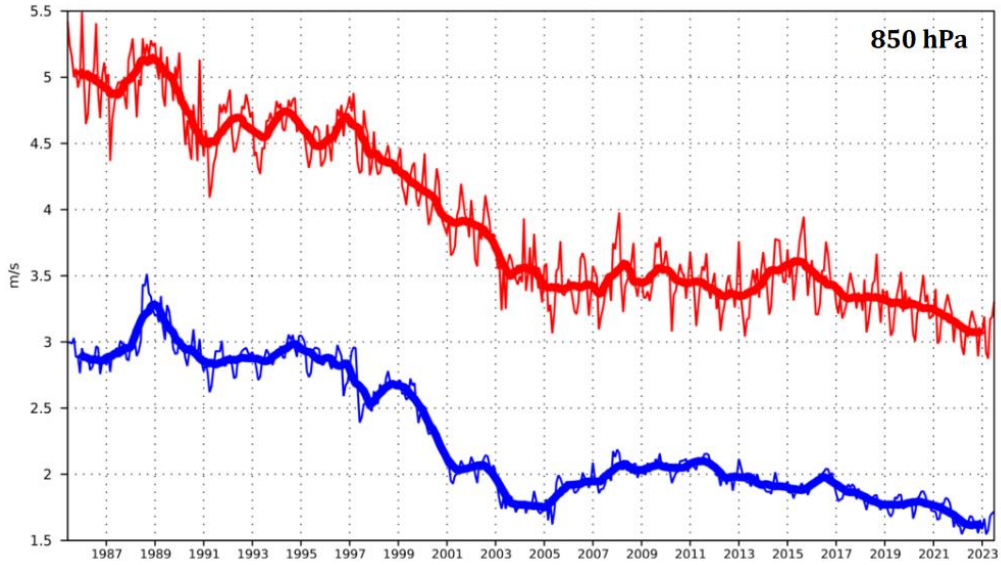

Figure 2. ECMWF forecast performance. Monthly wind speed root mean square error (RMSE) at 850 hPa for one-day (blue) and five-days (red) time horizon forecast. Bold lines represent a 12-month moving average of the results (figure extracted from [23]).

There are two major groups of NWP models: global models (grid covering all the Earth) and regional/mesoscale models (also known as limited area models) [24]. The main differences between these two groups are related to the spatial and temporal resolution of the model, the geographical area covered and the time horizon. Moreover, regional/mesoscale models are calibrated using physical parameterization for specific regions which can reduce the forecast errors. These differences will have a significant impact on forecast accuracy and computational effort [24]. Table 2 characterizes the spatial and temporal resolution of some of the existing global and mesoscale/regional model.

To overcome certain limitations inherent in global models characterized by low spatial and temporal resolutions, regional/mesoscale models can describe the behaviour and evolution of air masses, explicitly addressing atmospheric phenomena that require high spatial and temporal resolutions. Therefore, most of power forecast systems use a coupled approach by feeding the regional models with initial and boundary conditions (IBC) gathered from the global models. Numerical mesoscale/regional models always need to be forced with IBC at the limits of their domains (boundary, surface, and top of the domain), Figure 3. These IBC can be historical data from reanalysis projects (used to produce wind or irradiance atlases for example) or by operational global forecasts projects (as GFS).

Table 2. Example of global and regional models available. Adapted from [24].

Type of model	Provider	Model	Temporal resolution (hour)	Horizontal resolution (aprox. km)	Runs per day (UTC)
Global	European Centre for Medium-Range Weather Forecasts (ECMWF)	Integrated Forecasting System	1	10	4 (00, 06, 12 and 18)
	Canadian Meteorological Centre	Global Deterministic Prediction System	3	25	2 (00, 12)
	National Centers for Environmental Prediction	Global Forecast System (GFS)	3	25	4 (00, 06, 12 and 18)
	Deutscher Wetterdienst	Icosahedral Nonhydrostatic	1	13	4 (00, 06, 12 and 18)
Regional	Deutscher Wetterdienst	Consortium for Small-scale Modeling	1	2.8	8 (00, 02, …, 18 and 21)
	Finnish Meteorological Institute	High Resolution Limited Area Model	1	7.5	4 (00, 06, 12 and 18
		Weather Research and Forecasting (WRF)[1]	Defined by user (< 1 hour)	Defined by user (< 5 km)	User specific (but limited to the global model availability)

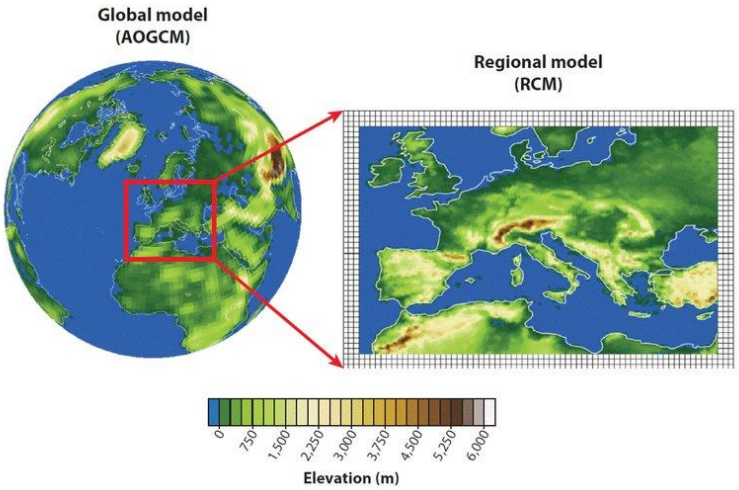

Figure 3. From global to mesoscale/regional numerical models (figure extracted from [25]).

[1] Example weather forecast providers using WRF model: Climetua (http://climeua.fis.ua.pt/weather) and MeteoGalicia (https://www.meteogalicia.gal).

Despite the improvement observed in NWP models, these models still present systematic errors partly explained by the: 1) inadequate model's physics parametrizations; 2) inability to handle sub-grid scale phenomena; 3) stochastic behaviour of the atmosphere and 4) uncertainty on IBC [24], [26]. Additionally, these models lack on the direct use of historical weather data to refine the underlying model. Although it is a very recent topic and, therefore, not included in the work developed in the TradeRES project, machine learning-based weather prediction (MLWP) models are nowadays emerging as an alternative to traditional NWP [27]. These models provide forecasts using historical data, including observations and analysis data using machine learning approaches. MLWP shows promise in improving forecast accuracy by capturing data patterns not easily represented in explicit equations. Additionally, MLWP offers opportunities for greater efficiency by enabling the use of modern deep learning hardware and achieving more favourable speed-accuracy trade-offs, as opposed to relying solely on supercomputers.

Recently, MLWP has proven effective in enhancing predictions in areas where traditional NWP is relatively weak, such as sub-seasonal heatwave forecasting and precipitation nowcasting from radar images. One example of MLWP is the GraphCast that outperforms the results from NWP [27]. This model operates by taking the two most recent states of Earth's weather, the current time and six hours earlier, as input and predicting the next state six hours ahead. Each weather state is represented by a 0.25° latitude/longitude grid (721 × 1440), translating to roughly 28 × 28 kilometre resolution at the equator. Like traditional numerical weather prediction systems, GraphCast is autoregressive, allowing it to generate an extended trajectory of weather states by feeding its own predictions back as input.

The precision of the results of NWP models increases proportionally to the number of data assimilated in these models, as well as the quality of these same data [24]. At the current stage of NWP, the model's parameterization and the spatial resolution from these models are unable to simulate some local effects as the exact location and extent of cloud fields in the case of solar power forecast. To properly account for these effects and correct the outputs from NWP, downscaling techniques can be applied to correct the data providing location-specific forecasts [28], [29]. Thus, downscaling consists of applying further methods to enhance the data extracted from the NWP with local/regional effects. This process can be performed through various statistical methods that establish relationships between local variables (such as wind speed) and variables with large-scale characteristics (such as pressure fields). Another possibility is the use of other physical approaches that varies according to the type of technology under consideration. Below, some examples of downscaling physical approaches for the wind and solar power cases are provided.

- Wind power

Microscale models: This type of model allows working with high spatial resolutions (up to 10 – 30 meters). With the growing need to estimate accurately the wind resource for different applications, new models for simulation of wind flow were developed. These models can be classified into linear and non-linear [30]. Linear models as the Wind Atlas Analysis and Application Program software have the advantage of low need for computing resources and it enables to evaluate, with reasonable accuracy, the wind resource for flat

orography with small elevations, *i.e.*, under non-complex terrain conditions [22]. However, these models tend to, *e.g.*, miscalculate the wind speed behaviour in the lee side of the hills [30]. Therefore, these models are unsuitable for complex terrain. The advances in numerical modelling together with the increase in computational capabilities enabled the development of non-linear models in the flow simulation industry and in the assessment of wind potential. Among these non-linear models, in the wind sector, computational fluid dynamics (CFD) models stand out enabling to increase the accuracy of wind potential assessments, especially in complex terrain [31]. Results from several authors highlighted the benefits of this model against the linear models [32]. These benefits are derived from the inclusion of thermal effects in the vertical stratification of the CFD simulations. This type of approach was explored in [33] showing higher performance when compared to a traditional statistical approach, especially for periods with high or low energy levels and in the ascending wind power ramps.

Conversion to power: This type of approach is based on the power curves from the wind turbine manufacturers/or estimated based on historical wind speed and power data to determine the power from the wind turbine or park [34]. Typically, the historical power curves of wind turbines/parks are defined as a function of additional parameters, such as wind direction to account for physical features (e.g., wake effect of wind turbines, air density and terrain) in surrounding regions [34]–[36]. Based on the results of the NWP, namely, the wind speed and direction for the hub height of the wind turbine, the power curves are applied, and the forecast is obtained. This type of approach is the most common during the initial periods of wind park operation where there is no historical data.

Figure 4 presents the main steps commonly applied to obtain the physical-based wind power forecast.

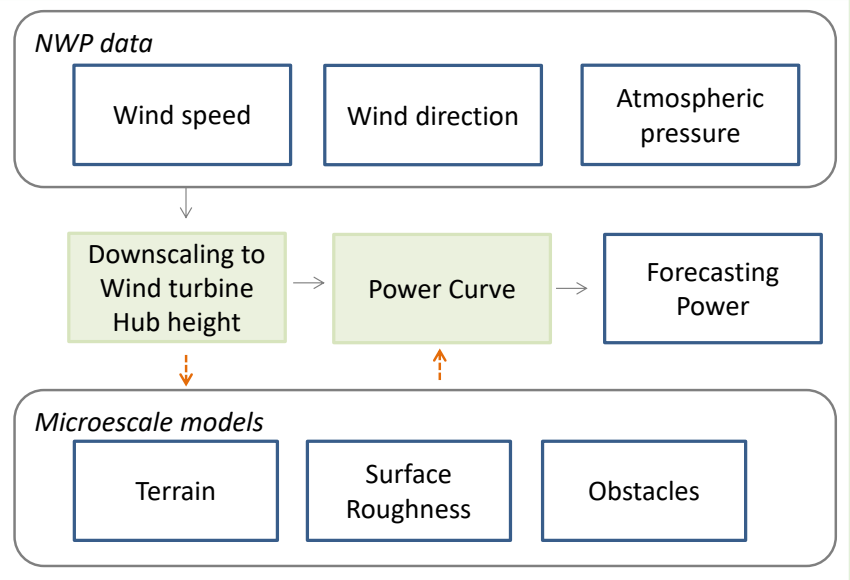

Figure 4. Main steps applied in the physical wind power forecast approaches. Orange arrows represent alternative approaches that can be used.

- Solar power

Cloud and all-sky imagery: In addition to the daily cycle, the other factor with the greatest impact on ground-level solar irradiation and, consequently, on solar production is the cloud cover [37]. This parameter presents a high variability that can be induced by local effects, which are not always correctly described by NWP. In recent years, models that forecast cloud cover from images from the sky taken from all-sky cameras or by artificial satellites have been developed. The all-sky cameras, installed at ground level, allow to obtain images of the sky, being very useful for very short and short-term forecast time horizons due to the reduced field of view of the camera [38], [39]. On the other hand, through satellites, it is possible to obtain images with a wide field of view, but with lower spatial and temporal resolution. In this sense, information obtained through satellites is more suitable for short and medium-term forecasts [40]. Regardless of the source of information (cameras or satellite), this type of approach uses algorithms that identify cloud coverage patterns between sequential images. The information from the images can be transformed, for instance, into cloud motion vectors, enabling to determine the movements (intensity and direction) of individual clouds [41]. This information regarding the cloud cover can then be used in different ways: i) correct the NWP outputs, or ii) apply semi-empirical models to obtain ground level solar irradiance.

The use of these models is crucial for weather-dependent generation technologies as wind and solar power forecast. Nevertheless, the outputs from these models are also used by several authors to improve the load forecast for short- and medium-term forecast horizons [42].

2.3.2. Statistical and machine learning approaches

To overcome the inefficiencies of the physical methods described above and, at the same time, obtain operational forecasts with adequate precision to manage the variability of vRES, several statistical approaches have been developed. This type of forecasting approaches relies on historical time series data. More precisely, this type of approach seeks to establish relationships between historical data series with what is currently observed, at the instant for which the forecast is to be made. Despite the constant emerging of new forecast techniques that require deep mathematical knowledge, compared to physical forecasting methods, this type of method presents reduced complexity and is less costly (whether in terms of time or resources) since the physical processes are not explicitly treated. Within the statistical models, three distinct methods are usually considered: persistence, time series modelling, and machine learning methods.

*Persistence methods***:** Persistence-based forecasting methodology is the most basic and simplest statistical forecasting methodology to be implemented. Despite belonging to the group of statistical approaches, it is often addressed separately since it is considered as reference, or benchmark. In this sense, to study the feasibility of implementing new forecasting systems must be compared with the results achieved by the persistence method. Only methodologies that present more favourable results than those generated by persistence are considered suitable for implementation. The persistence method assumes that the wind/solar power or electricity demand, remains equal, at a future instant,

to the value observed at the instant for which a forecast is made. If the power, at time *t*, is given by p_t, then the power at the future time, *t+k*, will be given by:

$$p_{t+k} = p_t \quad (1)$$

where Δt corresponds to the time interval for which the forecast is to be performed. For very short forecast time horizons (as presented in Table 1), this model provides results, on average, with some accuracy. However, and as expected, due to the vRES variability for long forecast time horizon the accuracy of this methodology decreases. In the case of time series characterized by substantial fluctuations in production, such as those observed in wind parks situated in areas with complex terrain, the accuracy of this method may be diminished, even when forecasting for very short lead times.

Methods based on time series modelling: For very short and short forecast time horizons (Table 1), there is the possibility, with a certain degree of reliability, to use methods based exclusively on the statistical analysis of time series of real data. Specifically, this type of methodology tries to establish the relationship between a historical series of production or demand data, and its value at the instant for which the forecast is to be made, in order to obtain predictions for the following time steps. Unlike physical models, in this type of forecasting methodology, only one step is needed to convert the input data into output data. Some of the most common statistical methods used in power forecasting are: the autoregressive (AR), moving average (MA), autoregressive moving average (ARMA), autoregressive integrated moving average (ARIMA), the Box-Jenkins methodology, and the use of Kalman filters [1], [43].

Machine learning methods: Machine learning (ML) or "*black-box*" [44] are models essentially characterized by the capacity for self-learning through experience and training, *i.e.*, ML offers the computational capacity to learn from the past information without explicit programming. As such, ML algorithms present the possibility of learning and making predictions on a set of data in an unexplicit way without following a set of static statistical learning instructions. The process of a self-learning model includes a few steps.

Firstly, it is necessary to obtain data referring to the past for a training phase. Secondly, a relationship between the input and output data desired through a target function need to be defined. The third step is to choose the self-learning model. Then, this type of method undergoes a training process, using the set of data and previously determined examples. In most cases, this type of methodology generally presents the best forecast results. However, the implementation of these methodologies has the disadvantage that it is not possible to describe completely the relationship between the elements of the model, *i.e.*, it is not possible to describe or understand the relationships found by these models between the input variables and the output variables [45]. Nevertheless, for a comprehensive understanding of ML results, explainable artificial intelligence techniques (XAI), such as feature importance analysis can be used. The selection of XAI is partially related with the specific ML model employed [46] but all the techniques aim to increase the transparency and interpretability of the results, by, for instance, quantifying the importance of each input feature in the model [46], [47].

Among the methods of this group, the artificial neural networks (ANN) are one of the most used in power forecast systems due to their simplicity and efficiency. One of the disadvantages of statistical methods as multiple linear regression lies in the inability to deal with the occurrence of events with distinct patterns within the time series, namely, the distinction between weekly, weekend and special days (*e.g.*, holidays). ANN-based methods, on the other hand, can accept these characteristics as an independent variable and modelling implicit non-linear relationships between the forecast variable and the variables that affect it.

Various machine learning techniques frequently employed in power forecasting systems include: Random Forest (RF) [48], support vector machine (SVM), XGBoost [49] and LightGBM [50]. Random Forest is an ensemble of decision trees that effectively addresses complex relationships and overfitting. It utilizes bootstrap sampling and feature subsets to create multiple trees, combining their predictions for enhanced reliability. It is always a trustworthy algorithm because it offers good accuracy and feature insights but may be slow on larger datasets and require tuning. SVM constructs a hyperplane that best fits the data, aiming to minimize the difference between actual and predicted values. Its strength lies in its flexibility to handle both linear and non-linear relationships using kernel functions. Despite this versatility, the choice of the appropriate kernel can significantly impact model performance. SVM might not perform well on very large datasets due to its computational complexity. XGBoost is a gradient boosting algorithm that combines weak learners, typically decision trees, to create a strong predictive model. It optimizes an objective function by iteratively adding trees that correct the errors of previous iterations. Advantages include handling missing values and feature selection, ability to capture complex interactions, and regularization techniques to prevent overfitting. However, it demands careful hyperparameter tuning and might be computationally intensive for large datasets. LightGBM is an advanced gradient boosting algorithm. It constructs decision trees, emphasizing optimal splits grounded in features that yield significant reduction in the objective function. This strategy enhances efficiency by prioritizing informative features during initial tree development. LightGBM effectively manages extensive datasets through its refined tree growth approach, leading to reduced memory usage.

Table 3 resents a list of the most common statistical and learning approaches and their advantages/disadvantages.

Table 3. Characteristics of the most common forecasting methods [18], [51], [52].

Forecasting method	Advantages	Disadvantages
Linear Regression	Simplicity; You can use only one (Single) or several (Multiple) independent variables.	Only capture relationships between linearly correlated variables; Sensitive to extreme values (outliers); Variables used in forecasting must be linearly independent.
Time Series Analysis (Box-Jenkins)	Adaptable, there are many versions of the method and it has already been extensively studied; Able to deal with seasonality and non-stationarity.	Requires only historical data for the series; Unlikely to perform well in long-term forecasting; It is computationally demanding to estimate model parameters.
K-nearest neighbour (KNN)	It is relatively simple to understand and implement; It does not need a training phase, making its prediction based on observed historical values; Non-parametric approach no assumptions regarding the distribution of the variables to be predicted is assumed.	Requires an extensive period of historical data; Computationally demanding for large datasets.
Artificial Neural Networks	It is not necessary to know the relationship between dependent and independent variables; Capable to deal effectively with non-linear relationships; Capable to deal with the presence of noise in the dataset without significantly affecting the forecast result.	It is computationally demanding to train the neural network; Requires a large amount of historical data from independent variables; Do not result in a mathematical model with physical meaning.
Support Vector Machine	Adjustment of the adjustment parameter of the objective function helps to avoid over-fitting the training data (over-fitting); Use of the kernel trick, which maps the variable space to a non-linear vector space, allowing to capture non-linear relationships more efficiently.	It is difficult to define a “good” kernel function; Computationally demanding for large datasets.
Random Forest	Handles non-linear relationships and interactions well; Provides feature importance for interpretability of the results.	Computationally intensive for large datasets; Requires very carefully tuning of hyper-parameters.
LightGBM	Efficient gradient boosting framework, optimized for speed and performance; Handles large datasets efficiently; Capable of handling non-linear relationships.	Requires parameter tuning for optimal performance; May be sensitive to outliers.
XGBoost	Effective handling of missing data and outliers. Ability to capture complex interactions, and regularization techniques to prevent overfitting.	Sensitive to overfitting, requires parameter tuning; Computationally demanding for large datasets.

Figure 5 depicts an example of the main steps used to apply statistical forecast approaches. As can be seen in the figure for the case of wind power forecast typically only wind speed or/and power historical data are needed.

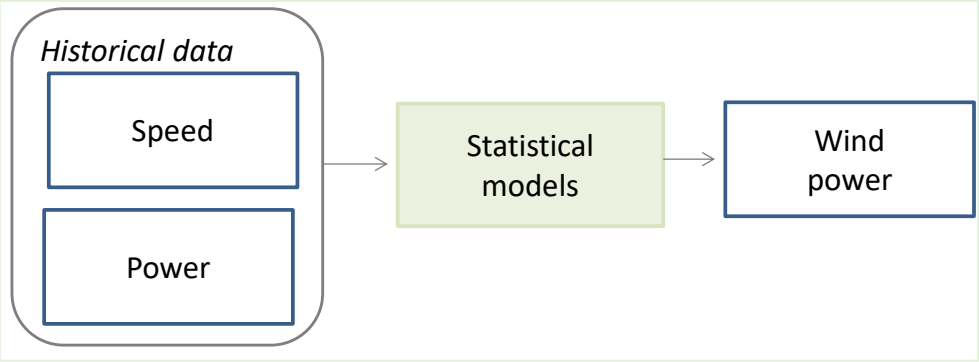

Figure 5. Example of the main steps applied in the statistical forecast approaches for wind power applications.

2.3.3. Hybrid approaches

Hybrid power forecast models are models that combine two or more models of similar or different nature [45]. The genesis of such approach results from the combination of both statistical and physical models. The time scales applicable to forecasting methods can also be different because it is possible to join methods whose forecast horizon is different. Hybrid models can be constituted by linear and a non-linear models to analyse the respective linear and non-linear components of the time series of data or it can be the combination of models with different source of information. Hybrid methods can be categorized into four different classes:

I. Weight-based methodologies: These methodologies are based on assigning weights to the various forecast models used according to their performance. It is a simple methodology, easy to implement and has the advantage of adapting to new datasets. It is a suitable methodology for a wide range of forecast time horizons. However, this does not guarantee the best forecasting efficiency for the entire forecasting time horizon and has the need for an additional model to assign the weights.

II. Methodologies based on the combination of different forecast approaches: the prediction is performed via the combination of different types of approaches (combine physical with statistical approaches). This type of methodology presents a robust behaviour due to the sudden, nature of the vRES generation wind speed. Therefore, it is possible to obtain high forecasting efficiencies. However, this type of methodologies has the disadvantage of requiring the user to understand the complex mathematical model that performs the data decomposition and the absence of a dynamic behaviour in the sense that the use of new data series, or the updating of the same, may result in a slow response of the methodology.

III. Methodologies based on optimization techniques and parameter selection: These methodologies are based on the optimization of the forecast model parameters – meteorological parameters such as temperature, wind speed and direction, precipitation,

among others. Despite providing the user with a greater understanding of the impact of different parameters on forecasting effectiveness, this approach is difficult to implement.

IV. Methodologies based on post-data processing techniques: These methodologies are based on a post-processing of forecast data. More specifically, this approach studies the impact of residual errors in the forecasts obtained, through the forecast models used, on the overall effectiveness. The effectiveness of forecasts considerably increased compared to other approaches. However, due to the need to calculate residual errors, computational and temporal resources required are much higher than those needed for the other approaches presented.

Figure 6 provides the main steps typically applied in hybrid power forecast approaches. Comparing with the previous approaches, it includes both NWP and historical data to feed the statistical models. As discussed in this section, for this type of approach different combinations can be used in the power forecast systems.

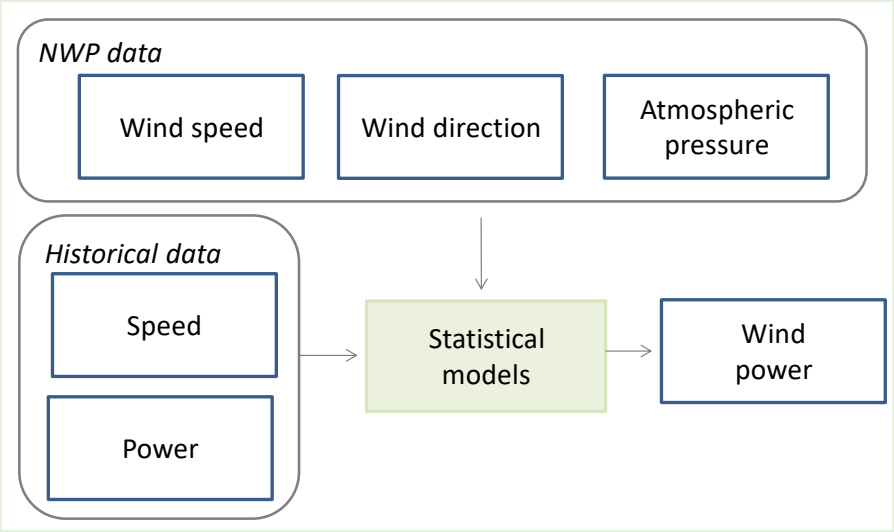

Figure 6. Main steps applied in the hybrid wind power forecast approaches based on a combination of different forecast approaches.

2.4 Data pre-processing

Before applying statistical forecasting methods, it is common to apply pre-processing procedures to the data under analysis [18], [53]–[55]. The most common types of pre-processing are data cleaning, integration, transformation, and dimensional reduction. These treatments can be used in various combinations or alone. Data cleaning consists of removing or modifying values from incorrect values and entering missing values. Integration consists of combining data from different sources. The transformation consists, for example, in normalizing the data to scale them on a predefined range (*e.g.*, [0, 1]) or in transforming a value recorded every 15 minutes into an hourly average.

Dimensional reduction consists of reducing the number of existing variables. This reduction can be done, for example, through principal component analysis (PCA), discriminant analysis, empirical mode decomposition or wavelet analysis [56]. In PCA, an orthog-

onal transformation is applied to convert the data into a set of values of linearly uncorrelated variables designated as principal components (PCs) [57]. With this procedure, the number of PCs generated in the process is always equal to or less than the number of original variables. The transformation applied with this technique allows the first PC to explain the largest possible variance, i.e., this PC characterizes the maximum possible variability observed in the data. With the restriction that it is orthogonal, the subsequent PC has the greatest possible variance that was not explained by the previous one. The process continues until the number of PCs became equal to the number of original variables. The resulting vectors enable to obtain an uncorrelated orthogonal basis set and they are used to feed the statistical forecasting techniques.

Another type of approach to reduce the data dimension is the application of feature selection algorithms [56]. The selection of the most relevant features aims to remove insignificant entries in the forecasting models allowing to reduce model complexity as well as computational costs [58]. These methods can be classified into three different types [55], [58]: filter, wrapper, and embedded. The filter methods remove the less significant variables *a priori*, and then a model is created with the remaining features. Variables are eliminated with a criterion such as Pearson correlation. The wrapping methods involve the entire training algorithm in the variable selection process. The algorithm runs with several iterations (as many as there are variables) of the model by adding (or removing) variables and evaluating the performance of the model obtained. For the construction of the final model, the variables that enable to improve the result are kept and the rest discarded. Embedded methods introduce the variable selection process directly into the training process, in order to avoid the complete search that happens in wrapped methods, thus reducing computational complexity [59]. Additionally, combinations of these methods can be created, giving rise to the so-called hybrid methods. All these techniques aim to ensure the robustness of the data, also bringing benefits in improving computational efficiency.

Another type of pre-processing is the decomposition and classification of data by clustering [56]. Decomposition, in the context of the analysis of electricity demand forecast refers to the data separation according to the seasonal, weekly, and special days (holidays) effects. For the vRES case, this classification can refer to the so-called weather regimes (WR) types [60] or target-circulation types (TCT) [61]. The WRs allow to reduce the complexity of meteorological variability while enabling the identification of daily recurrent patterns in the climate system (top-down approach). On the contrary, TCT are derived from the power system's weather response (down-top approach), which can be the vRES generation [62].

2.5 Forecast output: deterministic, probabilistic, or ramp events

The initial focus of power forecast systems was to provide deterministic information, i.e., a value for each time step of the temporal horizon. Famous statistical methods are ARMA, ARIMA, Kalman filtering and Gaussian mixture models [44], [63], [64]. Other robust statistical approaches include ANN, KNN among others [65]–[67], as discussed in the previous subsections. Deterministic forecast approaches do not include information regarding its uncertainty in the expected value, which can be very a very useful information for utilities or

for specific market players enabling the definition of strategic bidding [68]. The need to characterize and assess the uncertainty in the vRES power forecast to better integrate it in decision-making processes led to the development of various probabilistic forecasting techniques [69]–[73]. Probabilistic forecasts can allow: i) increase the revenues of market players within the electricity environments, *e.g.*, [74], [75], and ii) suitable reserve allocation [76].

Broadly speaking, the probabilistic forecast allows to obtain probability density functions (PDF) for a specific time providing an interval of uncertainty of future events. The PDF can be achieved using physical approaches (*e.g.*, NWP ensembles [77], [78]), statistical, or the combination of both. As described in [77], NWP ensembles forecasts are computationally demanding when compared with statistical methods. Power forecast uncertainty using statistical/hybrid models can be attained by calculating their distribution parameters based on: i) nonparametric regression assumptions as quantile regression [71] and kernel density estimators [79], [80], or ii) upon historical analogous [81]–[83] or iii) parametric distribution assumptions.

Ramp events refer to the significant changes of power output in a short period. Thus, the importance of the detection of severe power ramps for TSOs lies on the necessity to control conventional power plants to balance those ramps to ensure the stable operation of the power system. Contrary to deterministic and probabilistic forecast that provide time-series, this type of forecast provides binary information: existence or not of a power ramp [84]. This information should be integrated into the existing forecasting systems as an additional feature, but cannot substitute the existing forecasting systems [8]. Thus, the main potential benefit of power ramps forecast is to alert the TSO regarding the presence or absence of power (rapid) ramp events. This information enables the TSO to proactively allocate additional reserves, ensuring the safety and robustness of the power system under various meteorological conditions [8], [57].

Figure 7 schematically represent the different forecast outputs for deterministic, probabilistic and power ramp event cases,

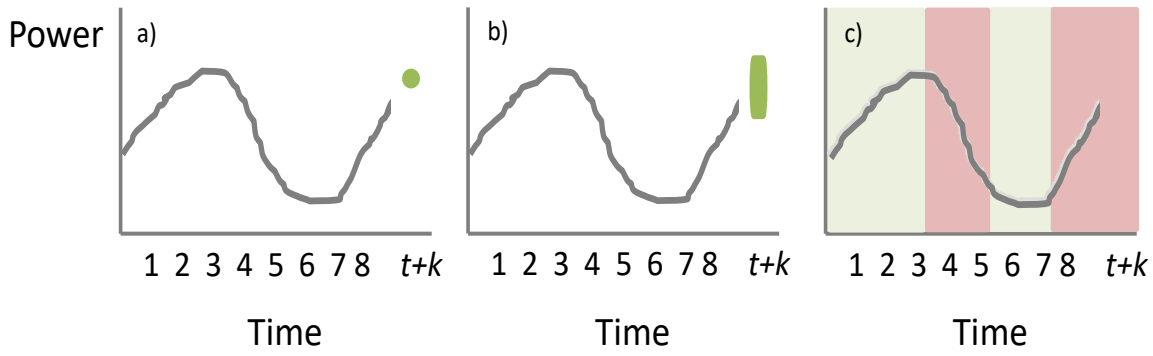

Figure 7. Different forecast outputs: a) deterministic (green point), b) probabilistic (green points), and c) ramp events (red background represents periods with severe power ramps and green background represents periods where power ramps are not expected).

2.6 Metrics to evaluate the performance of the forecast approaches

There is no single metric that can describe or measure the performance of a forecasting methodology. In existing literature, some new deterministic and probabilistic metrics have been proposed in the last years [85]. Nevertheless, most of them are not being adopted to energy sector being difficult to place the results among the values found in the literature. Taking into account this aspect, the following metrics will be used in TradeRES project to access the accuracy of time-series forecast - normalized bias (NB), RMSE or the normalized RMSE (NRMSE), the Pearson correlation coefficient (*r*) and the average value of the absolute forecast deviation ($\widehat{FD}$):

$$NB = \frac{\frac{1}{T}\sum_{t=1}^{T} Forecast(t) - Observed(t)}{NominalPower} \quad (2)$$

$$RMSE = \sqrt{\frac{\sum_{t=1}^{T}\left(Forecast(t) - Observed(t)\right)^2}{T}} \quad (3)$$

$$NRMSE = \frac{RMSE}{NominalPower} \quad (4)$$

$$NRMSE = \frac{RMSE}{\frac{\sum_{t=1}^{T} Observed(t)}{T}} \quad (5)$$

$$r = \frac{\sum\left(Forecast(t) - \overline{Forecast(t)}\right)\left(Observed(t) - \overline{Observed(t)}\right)}{\sqrt{\sum\left(Forecast(t) - \overline{Forecast(t)}\right)^2}\sqrt{\sum\left(Observed(t) - \overline{Observed(t)}\right)^2}} \quad (6)$$

$$\widehat{FD} = \frac{1}{T}\sum_{t=1}^{T}\frac{|Forecast(t) - Observed(t)|}{Observed(t)} \quad (7)$$

$NominalPower$ corresponds to the total nominal power of the control region or vRES power parks under analysis.

The bias corresponds to systematic error present in the forecast. This metric denotes an average error value for the forecast time horizon allowing to assess whether the forecasting methodology tends to underestimate or overestimate comparing with the observed values. Ideally, a bias is sought, for the time horizon, as close as possible to zero.

RMSE allows to identify the variation of amplitude errors, due to the squared nature of the differences. NRMSE, as aforementioned discussed, normalizes the RMSE for an easily comparison between different forecast approaches. In the existing literature, normalization can be performed by dividing the RMSE either by the nominal power (4) or by the average of the observed wind power production values (5), as employed in the results presented in this deliverable. The perfect score of the last two metric is also zero.

The correlation coefficient (6) measures the similarities between the obtained forecasts, for a forecast time horizon, and the observed value for the same time horizon. This coefficient varies between [-1 1]. A value close to zero means poor predictions, and the unit value represents perfect predictions. A value close to -1 means that the forecast is in

phase opposition. The average value of the absolute forecast deviation (7) allows to illustrate the mean forecast deviation in relation to the observed power.

When needed, to quantify the improvement of using the forecast methods proposed in TradeRES project, the approach followed in [83] is used for each metric:

$$\varepsilon(\%) = \left(1 - \frac{Forecast_{TradeRES}}{Forecast_{Benchmark}}\right) \times 100 \quad (8)$$

where $Forecast_{TradeRES}$ represents the results of a specific metric using the forecast method implemented in TradeRES project, and $Forecast_{Benchmark}$ represents the forecast results for the benchmarking approach (that will be defined according to each case study). A positive ε value indicates an improvement of the proposed forecast method. A negative value corresponds to an underperformance of the TradeRES forecast method.

Ramps power events refer to a dichotomous case, *i.e.*, the existence or not of a power ramp. For this type of approach, a contingency table are usually built to derive the results. In Table 4, true positive (TP) corresponds to the ramps forecasted with the proposed methodology that occurred; false positive (FP) corresponds to the ramps forecasted but do not occur; false negative (FN) corresponds to power ramp events that occurred but were not forecasted; and true negative (TN) corresponds to power ramps forecasted and observed.

Table 4. Key Schematic 2X2 contingency table for power ramp detection. Adapted from: [57].

Event Foreseen	**Event Observation**		**Total**
	Yes	**No**	
Yes	TP	FP	Foreseen Yes
No	FN	TN	Foreseen No
Total	Observed Yes	Observed No	N=TP+FP+FN+TN

From the contingency table, the following metrics can be computed: Bias Score (Bias), precision, the probability of detection (POD) and the Hanssen & Kuipers Skill Score (KSS):

$$Bias = \frac{TP + FP}{TP + FN} \quad (9)$$

$$Precision = \frac{TP}{TP + FP} \quad (10)$$

$$POD = \frac{TP}{TP + FN} \quad (11)$$

$$KSS = \frac{TP \times TN - FP \times FN}{(TP + FN) \times (FP + TN)} \quad (12)$$

The ideal score for the aforementioned metrics is 1. KSS ranges between 0 and 1 [86]. Bias, precision, and POD metrics enables to understand if the power ramps algorithm has the tendency to over foreseen (precision, POD and Bias Score > 1) or under foreseen (precision, POD and Bias Score < 1) the number of power ramp events.

3. Electricity markets time frames and power forecasts

This section focuses on the relationship between electricity market time frames and the errors associated with power forecasts. Alternative solutions under analysis in TradeRES, including a potential shift to more frequent trading sessions, are presented as a solution to better synchronize market operations with the distinctive characteristics of vRES aiming to enhance forecast accuracy and reduce the overall system costs.

3.1 Existing and alternative market designs addressed in the TradeRES project

The existing designs of most European electricity markets were defined during a conventional energy technology dominated period. These technologies can respond to the demand variability, they are easily adjustable and, if requested in due time, they can respond efficiently to operational set points. However, in addition to the negative environmental impacts of using fossil technologies, the marginal cost to operate these technologies is high. In contrast, vRES are weather dependent and still present significant forecast errors, especially for long time horizons.

DAMs require the forecast of electricity production 12-36 hours before physical delivery in central Europe due to coupled DAM auction at noon, or 13-37 hours in Great Britain[2], Ireland and Portugal. This time gap between bidding and the first deliverable can jeopardize the profitability of vRES [87]. The DAM shortcomings and alternative designs for a near 100% renewable electricity system were addressed in different editions of Deliverable 3.5 from TradeRES project [5], [6]. The authors suggested a reduction of the time gap between the DAM closure and the delivery time. This reduction could facilitate vRES, since it allows reducing the uncertainty associated to power forecasts, and many flexibility options. The authors concluded that the "*choice for European market design is whether to maintain the current organization of wholesale electricity trade, in which the 24 hours of each day are traded together at noon the day before, or to replace it with a different wholesale market design*."

As shown in Figure 8 and Figure 9, for a time horizon above six hours, NWP-based forecast is the recommended approach for vRES technologies. Nevertheless, the forecast performance is worse than the one expected for very short and short time horizons. In [88], the authors quantify the annual value of using solar power forecast in the Iberian electricity market. The forecast models that use NWP data showed the highest revenue. The benefits from using an NWP-based forecast approach, with respect to the persistence prediction, ranges from 1 to 6 kEUR *per* MW of PV capacity *per* year.

[2] For Great Britain, the Day-ahead auction for 60 min products has been moved to 9.20 due to the Brexit, even enlarging the lead times. In addition, there is a 30 min auction held at 15.30.

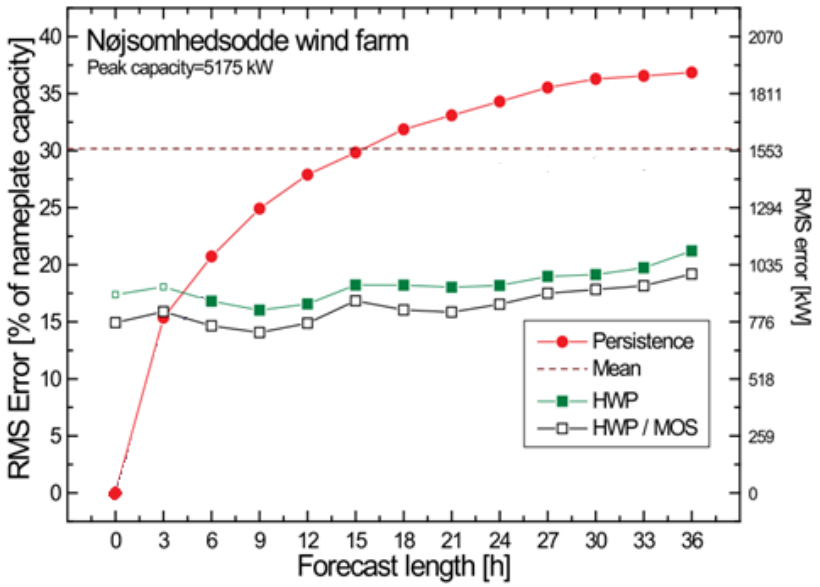

Figure 8. Forecast errors according to time horizon for different wind power forecast approaches. HWP approach refers to a physical approach and "HWP/MOS" refers to a hybrid forecast approach. Figure adapted from [37].

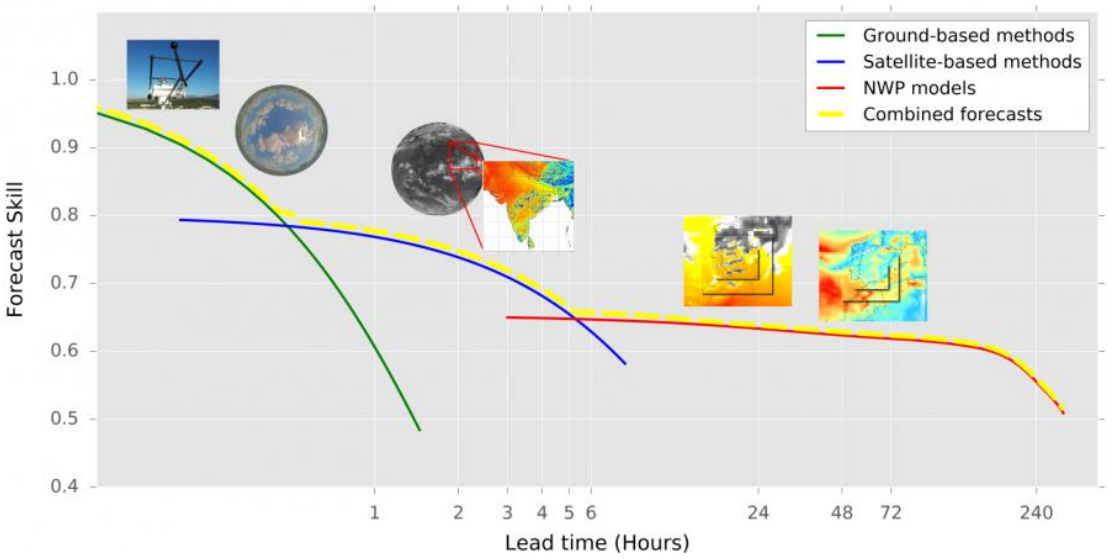

Figure 9. Solar power forecast skills according to time horizon and type of forecast approach. Figure extracted [89].

From a forecast point of view, the main motivation for the DAM closure change is related to the availability of the IBC conditions used to feed the NWP models. As mentioned in section 2, the quality of the power forecast strongly relies on these data. Most of the IBC availability from global models is limited to updates every 6 hours (at 00, 06, 12 and 18 UTC). To participate in DAM in Europe, the NWP-based power forecast systems currently use the IBC from 00 or 06 UTC to obtain the expected vRES production or electricity demand. To benefit from updated IBC data, postponing the DAM closure gate in some hours

could allow it to keep its overall structure, while it is expected to reduce the forecast errors. Figure 10 presents possible alternatives to use updated IBC data, while the 24-hour block of the DAM is maintained. The possible new gate closure hour is associated with the IBC delivery hour plus an additional two hours to perform all required steps (download the IBC data, run the numerical mesoscale/regional model and apply the different forecast approach) to obtain the forecast.

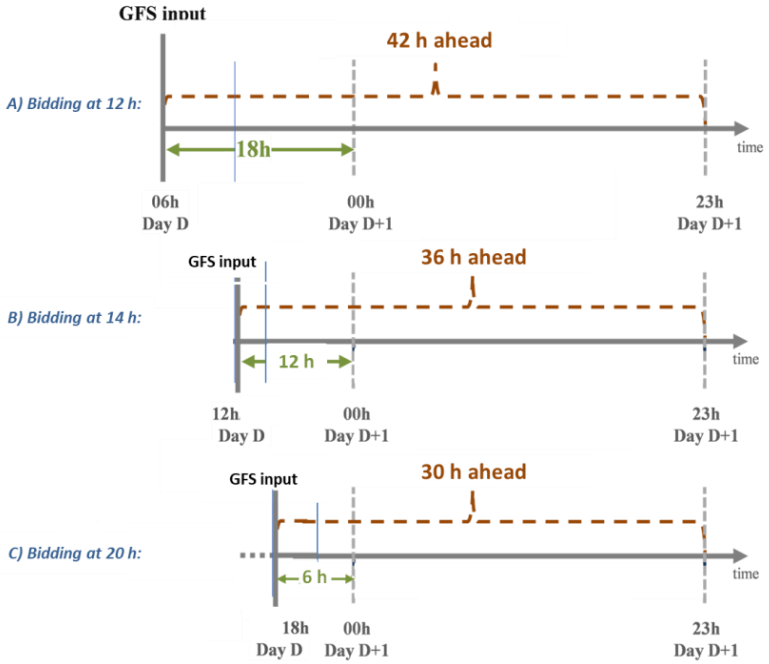

Figure 10. Possible DAM time frames taking in to account the meteorological data availability. D represents the day on which the simulation is carried out (Figure extracted from [90]).

In this energy transition phase toward a near 100% renewable power system, this postponing does not require any disruptive change in the market designs and, as described in Deliverable 3.5 [5], it can allow a "*compromise between the need to accommodate facilities with ramping constraints, which need longer lead times, and variable renewable energy sources, for which a short time between market clearing and delivery reduces weather uncertainty*".

In the current market design, market participants can already make use of short-term forecasts with high accuracy on intraday markets (IDM). Compared to the DAM design, intraday market designs show a larger variability across European countries. There are some (opening) auctions held on the day before delivery for some countries, such as the IDM auction for Austria, Belgium, Denmark, and Netherlands at 15:00 in which 15 min products are traded. For the continuous trading, a greater degree of harmonization has been established from the Single Intraday Coupling (SIDC) (see [91] and also TradeRES D3.5 [6]). Continuous intraday markets allow a trading up until real-time for Finland. For other markets, lead times are rather short and range from 5 mins for Austria, Belgium, Denmark and Netherlands to 30 mins for France and Switzerland [91].

Improved forecasting accuracy can lead to smaller asymmetry for balance responsible parties (BRPs), ultimately reducing their imbalance payments. Thus, there is already a

benefit of increasing generation forecast quality which will be further increased with trading even closer to lead time, potentially also in DAM markets, as well as rising shares of vRES.

The second edition of D3.5 from TradeRES project [6] introduces alternatives to the existing DAM market design, proposing a transition to more frequent trading sessions with shorter time horizons. In a system with nearly 100% RES, this market design aims to facilitate the integration of vRES by providing more accurate forecasts, thereby reducing the overall system costs. This shift aligns market operations with the intrinsic features of vRES, fostering a responsive, adaptable, and efficient energy market. Additionally, it can promote grid flexibility and the emergence of technologies and innovative solutions capable of providing the necessary flexibility. Figure 11 presents an alternative explored in the TradeRES project: the Period-Ahead Market (PAM), involving forecasts for 6 hours ahead with four updates during the day. As depicted in Figure 8 and Figure 9, implementing this shift may necessitate the adoption of new forecast systems since, for this timeframe, NWP-based models commonly used for DAM may exhibit inferior performance compared to models relying only on historical data (autoregressive).

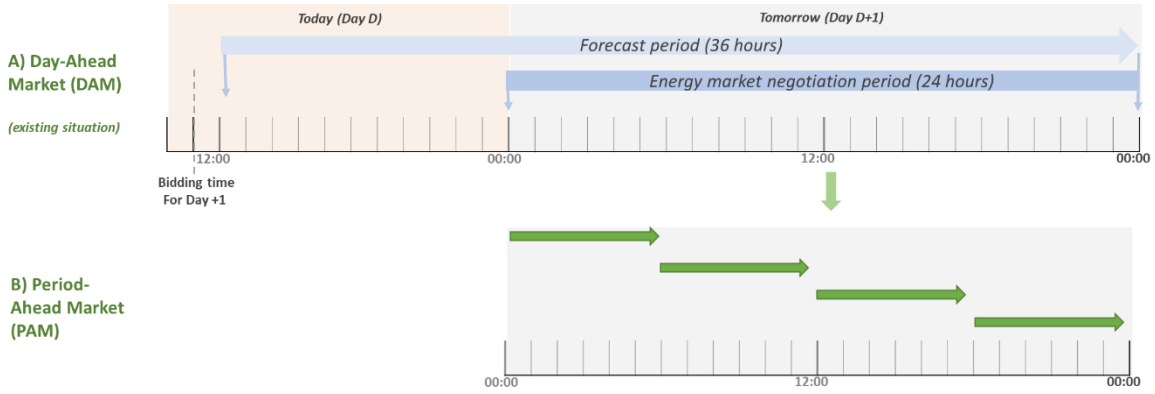

Figure 11. Schematic representation of day-ahead market and period-ahead time frames.

3.2 Impact on power forecast errors in market modelling

3.2.1. Modelling forecast errors in AMIRIS

Following the approach presented in Deliverable 4.1 from the TradeRES project [90], the Agent-based Market model for the Investigation of Renewable and Integrated energy Systems (AMIRIS) was enhanced to consider power forecast errors for agents marketing renewable energy. Since error distribution functions for different technologies and varying gate closure lead times are not yet fully integrated, a Gaussian distribution was chosen to represent the forecast error. The distribution parameters are exemplary and were selected to illustrate the impact of forecast errors on the market simulations and to demonstrate the basic functionality developed within TradeRES. The data used does, however, not yet represent realistic data regarding power forecast errors. The integration of realistic data will be completed in a subsequent step.

In this demonstration of the approach, the renewable energy trading agent was configured to consider power forecast errors with a constant distribution function over time. Thus, each hour of the day was assumed to follow the same error distribution. It is assumed that the power forecast error follows a normal distribution formulation. Generated values represent levels with different relative error. To obtain power supply bids that include these errors, the error level is multiplied with the perfect foresight power infeed (see also Section 3.3.1.2 in Deliverable 4.1 [90]) which can be extracted from historical time series data. Figure 12 shows the incidence of actual power forecast error levels obtained within AMIRIS. The normal distribution of the error levels is clearly visible. The positive mean of the distribution (13) corresponds to an average overestimation of renewable power. Due to the variance of the distribution (14), however, also negative error values occur, reflecting a lower-than-actual feed-in estimate.

$$\mu = 0.05 \tag{13}$$

$$\sigma^2 = 0.1 \tag{14}$$

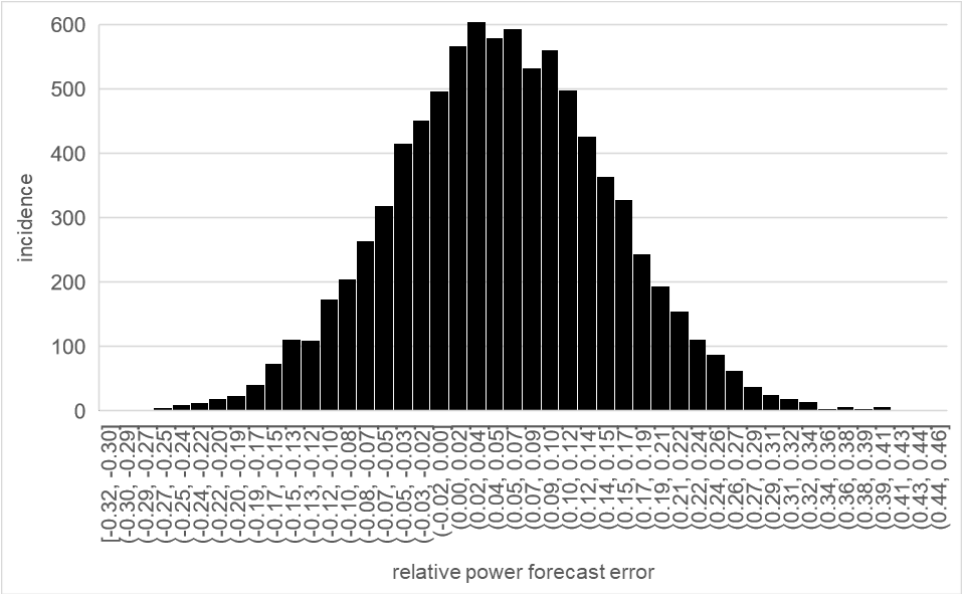

Figure 12. Histogram of relative power forecast error levels created in AMIRIS following a normal distribution with a mean of 0.05 and a standard deviation of 0.1; 8760 hourly data points representing one year.

The power forecast errors are created during the bid preparation stage of AMIRIS and propagate through the simulation. Therefore, these errors can impact the day-ahead market clearing price, traders' profits, and system costs as well as other subsequent markets (e.g., intra-day, ancillary services) which are not explicitly modelled in AMIRIS. Figure 13 demonstrates the possible impact of power forecast errors on the day-ahead electricity market clearing price using the same error distribution as before. For most situations, prices found with erroneous forecasts are below the "perfect foresight" prices that do not contain any forecast errors. This matches the expectation since an on-average higher renewable feed-in should lead to lower prices due to the merit-order effect [92].

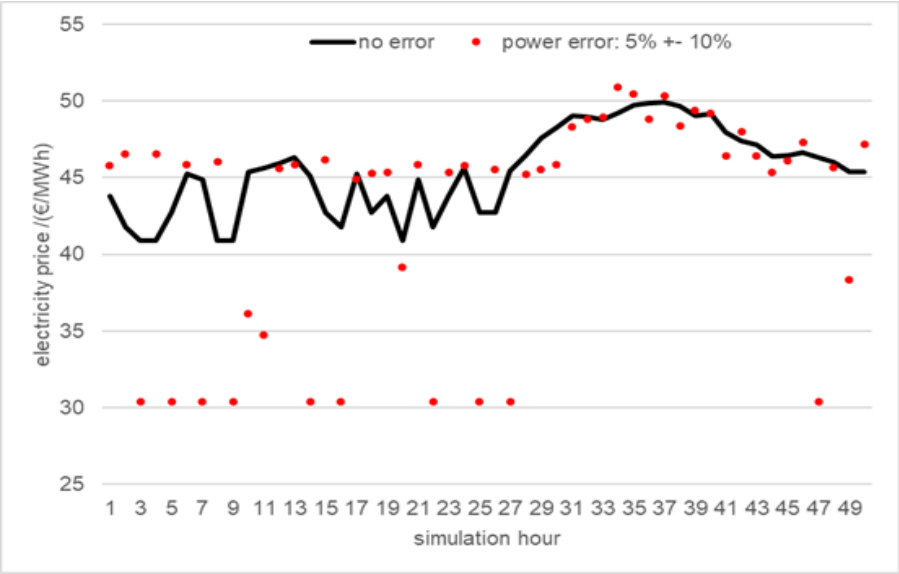

Figure 13. Sample impact of power forecast errors on (non-realistic) DAM clearing prices; black curve represents prices without power forecast errors, red dots resemble prices that include modified renewable feed-in estimates based on the same error distribution function as shown in Figure 12.

This simple example highlights the possible impact of power forecast errors on the market prices. It must be noted that several aspects are not yet satisfyingly reflected. For instance, real-world forecast errors might depend on the specific type of technology and the hour of the day. In addition, the errors shown here have no autocorrelation, while real-world error series often have autocorrelative features. Thus, to obtain a more realistic time series of errors, correlations should also be considered. Therefore, real forecast data developed in TradeRES will also be integrated into AMIRIS and their effects analysed within the scope of WP 5 activities. Although, a brief analysis is provided in the next subsection.

3.2.2. Impact of forecast errors in the simulation of German day-ahead market

The assessment of the value of perfect RES forecasting compared to a real forecasting has been conducted using AMIRIS. The German day-ahead market in 2019 was simulated for two erroneous forecasting cases for onshore wind infeed and compared to a reference run with no forecast errors:

1. *Reference – no errors*: The first case was the reference with no errors (i.e., the observed power generation in 2019), representing a perfect forecast of RES infeed.
2. *Forecast time series*: The second case involved a time series of forecasted onshore wind infeed with realistic errors.
3. *Gaussian errors*: The third case used errors of onshore wind infeed forecasting that follow a normal distribution applied to the observed power generation in 2019.

The case *forecast time series* uses power forecasts for wind onshore that underlie a 6-hourly updated forecast. The forecast time series has been generated by Enlitia for the year 2019 with hourly resolution using the methodology presented in [93] and in the fol-

lowing sections. The histogram in Figure 14 visualises the distribution of forecast errors throughout the year, relative to the actual infeed. Negative values indicate an underestimation of the feed-in. Low negative forecast errors are the most frequent. However, the distribution is skewed to the right, with some hours showing significant overestimates of the feed-in.

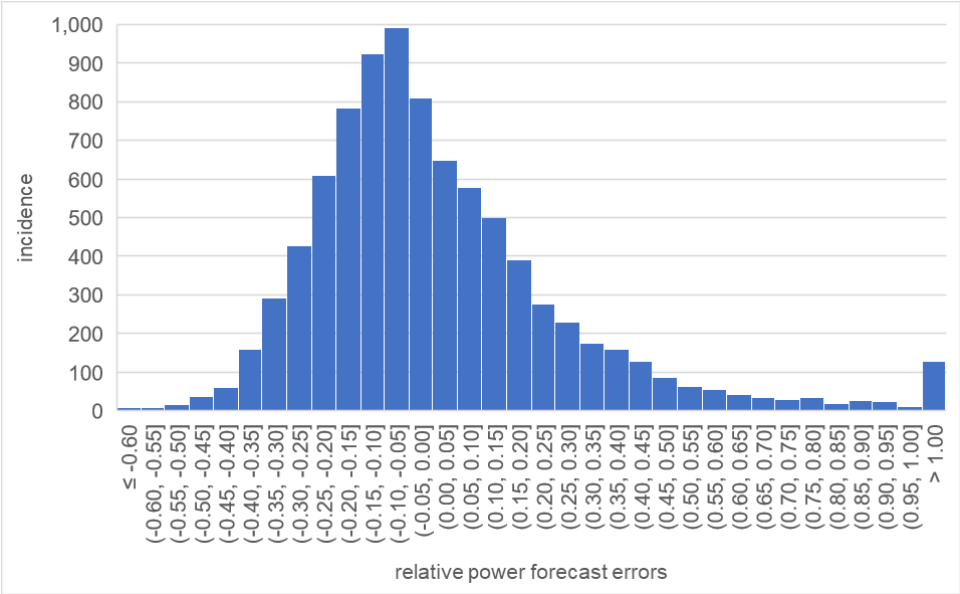

Figure 14. Histogram of hourly forecast errors in 2019 relative to the actual infeed, case *forecast time series*. Negative values indicate an underestimation of the feed-in.

The third case, *Gaussian errors*, follows the approach developed and described in section 3.2.1. The normal distribution was modelled on the forecast errors from the *forecast time series* case: the parameters μ and σ^2 were selected to ensure that the resulting error distribution closely resembles the one of the *forecast time series*. As a result, the forecast errors are similar to the case *forecast time series*, but there are no more extreme outliers in the *Gaussian forecasting* case and any autocorrelations are removed.

Figure 15 displays the predicted infeed capacity of onshore wind turbines in Germany for a winter week, considering the three types of forecasts. It is assumed that the wind traders offer their predicted (and possibly erroneous) power on the day-ahead market.

The forecast's quality was evaluated by comparing the awarded power as well as profits of wind onshore operators in the three depicted cases. Revenues from the day-ahead market as well as from support were calculated from the AMIRIS runs and aggregated for all wind onshore operators throughout 2019. Support for onshore wind operators was assumed to be in the form of a one-way Contract for Differences, with the levelized cost of electricity assumed to be independent of the forecast error case. It is important to note that the intraday market is not modelled in AMIRIS. Instead, if there is an underestimation of the feed-in (i.e. negative forecast errors), balancing energy costs apply. Balancing energy costs in case of negative forecast errors have been calculated based on historical balancing energy prices.

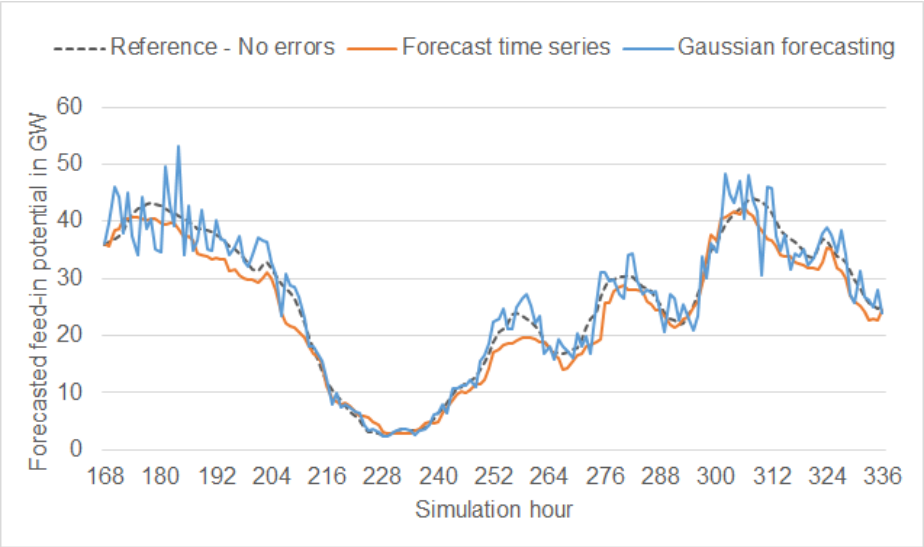

Figure 15. Forecasted feed-in potential of wind onshore for a winter week in Germany for different forecasting types.

Figure 16 illustrates the total power awarded at the German day-ahead market by onshore wind. The results show that in the *forecast time series* case, the awarded power is approximately 6% lower compared to the reference. This suggests that feed-in is underestimated based on the underlying error time series. In the *Gaussian forecasting* case, there is little difference compared to the reference.

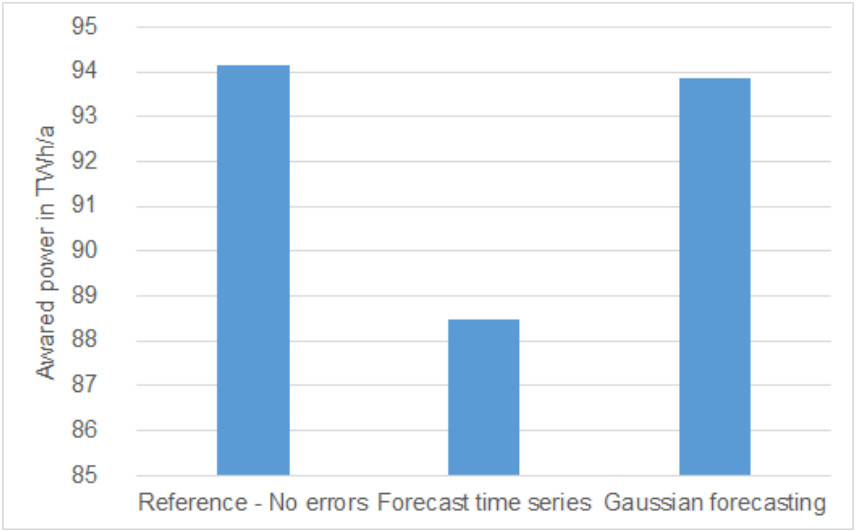

Figure 16. Total awarded power by onshore wind generators at the German day-ahead market for three different forecast errors.

Figure 17 shows the aggregated market revenues, support revenues and balancing energy costs as well as resulting net profits for different forecast error cases. The results indicate a significant decrease in profit for the *forecast time series* case, amounting to 700 million EUR less per year compared to the reference case. This decrease is mainly due to a reduction in support revenues, which are about 580 million EUR less per year than in

the reference case. In the *forecast time series* case, approximately 175 million EUR per year must be paid at the balancing energy market. Losses in the *Gaussian forecasting* case are smaller, with profits only about 435 million EUR per year lower than the reference. Balancing energy costs in this case amount to approximately 115 million EUR per year.

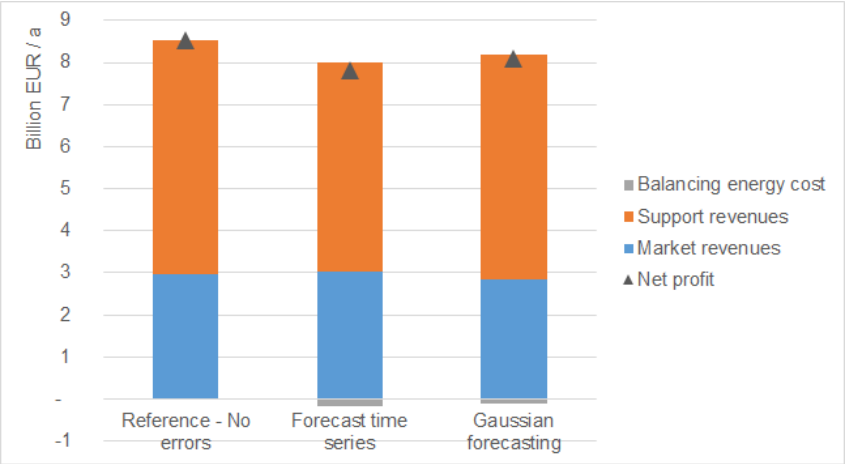

Figure 17. Aggregated revenues, balancing energy cost and net profit for wind onshore generators for different forecast errors.

To understand the reduction of support payments to onshore wind generators in the *forecast time series* case, one must examine market values. With less total awarded power by onshore wind due to the underlying erroneous forecast time series, both market prices and market values increase in the day-ahead market compared to the reference (see Figure 18). Consequently, the market premium, which bridges the gap between market values and the total levelized cost of electricity, decreases.

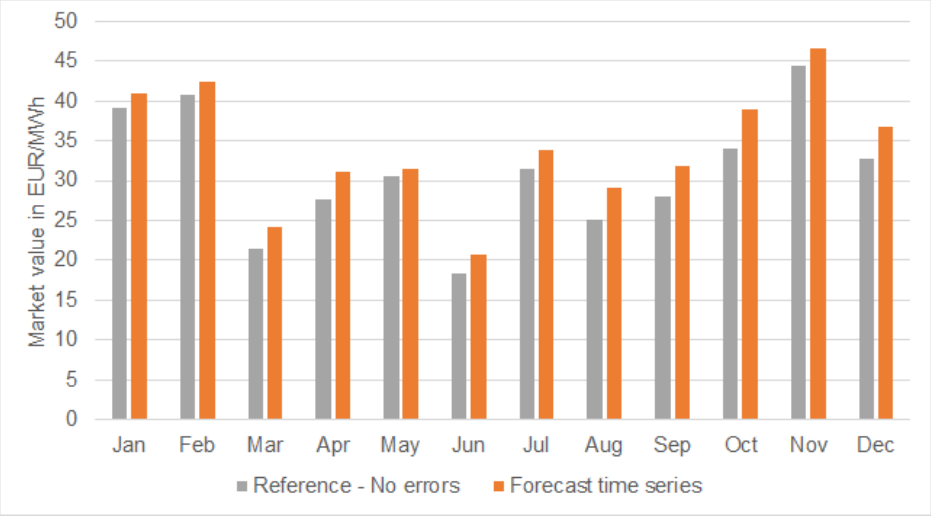

Figure 18. Monthly market values for wind onshore for the *forecast time series* case compared to the reference.

In summary, it should be noted that the errors discussed here are largely hypothetical. By eliminating extreme errors, the Gaussian-distributed errors should be considered a conservative estimate, while the error time series should be considered an upper limit for realistic errors due to its approximation of the German federal territory. The true forecasting error and its impact on the market trend remain unclear. Future research could aim to model more realistic forecast errors for different plant regions in Germany and quantify their impact on the overall market.

4. Forecast approaches developed in TradeRES project

In this section, some preliminary results are presented as a drive for the development of TradeRES vRES power forecast tools. Specifications of the market players/agents that will benefit from these forecasts are also presented. Results from the application of the tools are presented in the section 5 and it will be further analysed from a market perspective in the deliverable 5.3 - *Performance assessment of current and new market designs and trading mechanisms for National and Regional Markets* from WP5.

4.1 Deterministic vRES power forecast

As discussed in the previous sections, and supported by several authors (*e.g.*, [94]–[96]) the vRES power forecast accuracy for short and medium time horizons strongly relies on the outcomes of NWP model. The main error in the final forecast comes from the meteorological input rather than the existing statistical techniques applied in power forecast systems [94]. For instance, using one source of meteorology for wind speed forecast the mean absolute percentage error (MAPE) is approximately 15%. Using this wind speed as input, MAPE for wind power forecast is approximately 23%. However, using the same algorithm with another source of meteorology, with wind speed MAPE of 24%, the MAPE error for power forecast has a substantial increase, around 45%. A generic graphical representation of a generation modern wind turbine power curve, which presents typically a cubic dependency of wind speed for the range between 4-11 m/s. For these wind speed ranges, one can intuitively understand that an absolute error of 1 m/s in wind speed can represent a high error value in power forecast. However, the full potential of the output of NWP models was not fully explored. For instance, most of the vRES power system systems use a single point information from the NWP grid and a limited number of meteorological parameters.

For the specific case of the single point outputs, the variability in generation observed in a given wind or solar power plant depends not only on the local dynamics, but it is also influenced by large-scale atmospheric patterns [83]. Although these patterns may be well simulated, in a specific location, the time series may present deviations [97]. Thus, another feature of the NWP that is not usually explored in forecasting systems is the use of the results of a spatial grid in contrast to the use of only data from a single spatial point or the midpoints of the NWP domain surrounding a wind power plant/ solar PV [98]. In [83], a methodology that combines a gradient boosting trees algorithm with feature engineering techniques, aiming to extract the maximum spatial and temporal information from the NWP grid to improve wind and solar power, was implemented. The authors identified that the use of PCA enables to improve the wind power forecast accuracy. Thus, the achieved results indicate that an adequate extraction of features from the raw data of the NWP can improve the forecast systems. The authors recommend more investment in the data mining phase as well as the application of statistical downscaling techniques capable of incorporating all data.

Regarding the meteorological parameters extracted from NWP, recent works have shown that a careful selection of input variables for statistical methods can improve the

accuracy of the wind and solar power forecasts [56], [59], [95], [96]. In the case of wind power, the most common meteorological parameters used as input to feed the downscaling approaches are the wind speed and direction. The influence of parameters related to the conversion efficiency as air temperature and pressure are included in some works. In [97] the authors included parameters from the upper levels of the atmosphere (e.g., the 850 and 500 hPa pressure levels) as input to improve the performance of the statistical models. Using a PCA, in the work conducted by [99], the following parameters were identified as the most relevant to forecast the wind power variability: mean sea level pressure, geopotential height, and the meridional wind component and humidity relative. A physics-oriented pre-processing with a NWP feature selection approach had a positive impact on the model performance from the team that won the European Energy Market Conference competition [100]. In [56], the author identified that a possible development trend to improve the power forecast systems is to include exogenous meteorological input variables. Using seven wind parks in Portugal [95], the authores demonstrated for seven wind parks that the optimal selection of meteorological data used in the forecast can lead to a reduction in wind power errors ranging from 13 to 37%. The authors showed that parameters as wind gust, wind power density, wind shear, and planetary boundary layer should be used to improve the wind power forecast. The authors also demonstrate the benefit of using NWP grid-spatial data against the use of NWP point data. For using the grid-spatial data, the authors applied PCA technique. By applying the PCA and a sequential forward feature selection algorithm (SFF) the RMSE can be reduced by nearly 25% compared to the benchmarking approach (single-point forecast with a limited number of meteorological parameters), Figure 19. If only PCA is applied, the results show a reduction in the RMSE values of nearly 8%. Although the use of PCA improves the forecast, an insightful selection of the meteorological features is paramount to reduce the uncertainty in the wind power forecasts.

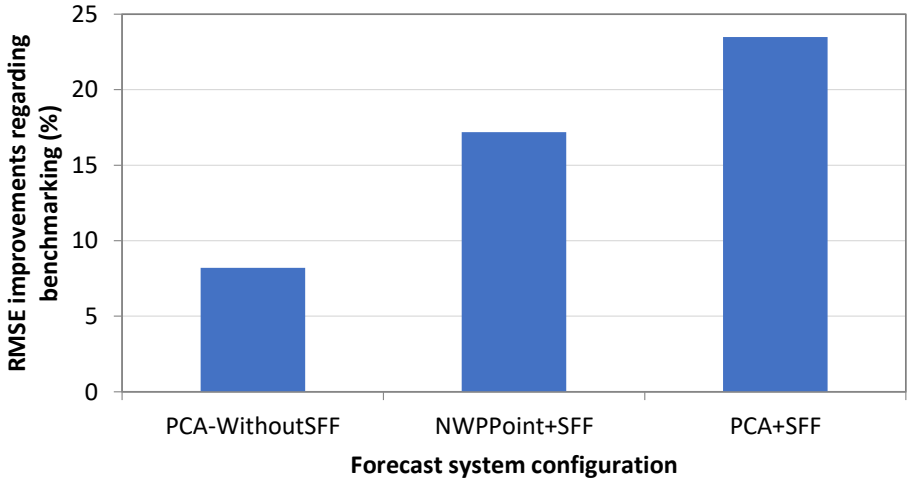

Figure 19. Average RMSE improvements for the seven wind parks analysed compared with the benchmarking approach. “PCA-WithoutSFF” – PCA approach without applying SFF algorithm; “NWPPoint+SFF” – data from NWP was extracted to the nearest point of each wind park and the SFF was applied; “PCA+SFF” – PCA approach and application of the SFF algorithm.

For solar power, [55] identified that parameters as precipitation intensity and wind speed penalized the performance of the forecast. On the other hand, parameters as ultraviolet index, wind bearing, and dew point could allow to improve the solar power forecast. In [101], the authors observed that the selection of features plays a more important role than the choice of the machine learning models in achieving the most accurate results. Furthermore, in [102] the authors highlighted the significance of meteorological features such as cloud cover and relative humidity in improving solar PV forecasts.

Against this background, in TradeRES, a method was implemented to identify if the inclusion of meteorological parameters derived directly from an NWP and others with impact in wind and solar power generation behaviour. These meteorological parameters include both, surface (*e.g.*, planetary boundary layer) and vertical levels information. In addition, as discussed in section 3, short lead time forecasts based on historical data can suppress the performance of NWP-based forecasts. In this sense, autoregressive approaches were also implemented in the project and presented in the next subsections.

4.1.1. TradeRES NWP-based power forecast approach

In recent times, researchers have been focusing mainly on developing advanced statistical methods as a way to improve the power forecast approaches using machine learning and deep learning models [103]. These models, although powerful, present challenges due to their complexity and the need for extensive hyper parameter tuning [101], making them difficult to interpret and implement. Moreover, the observed performance improvements from some of these models are often marginal and are limited to specific case studies, raising questions regarding their universal applicability versus representing local effects. Another critical aspect is the selection of meteorological parameters used as input data for NWP-based power forecast systems [95]. While many studies focus on the development of statistical methods, they often overlook the potential of NWP information to improve forecast accuracy. NWP models offer various meteorological parameters that can be utilized as inputs. Typically, wind speed and direction are common input variables in forecast systems, but other parameters like air pressure, wind shear, temperature, and humidity, which influence conversion efficiency, can also be incorporated to improve the final results.

Based on this background, the vRES power forecast approach development within the scope of the TradeRES project aims to obtain the optimal combination of a large number of meteorological parameters using statistical and machine learning approaches, such as dimensionality reduction and feature selection algorithms, *prior* to applying several regression algorithms calibrated for different weather regimes. Based on the preliminary results, the main steps of the NWP-based vRES power forecast method applied in TradeRES are presented in Figure 20.

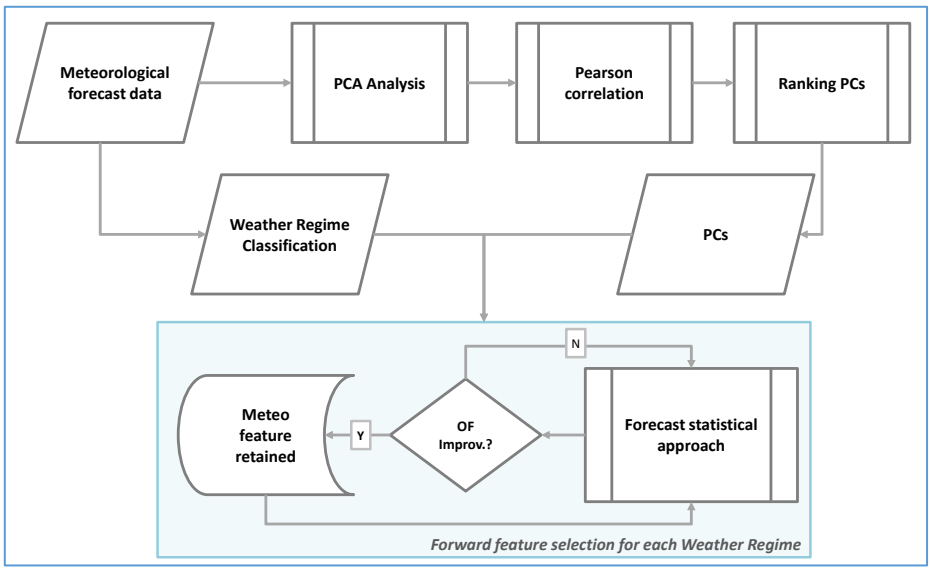

Figure 20. NWP-based power forecast approach implemented in TradeRES project.

The forecasting approach is also based on a SFF algorithm but, in this case, a calibration procedure according to the different weather regimes is performed. The classification of atmospheric circulation states into distinct types is a common approach used for understanding and scrutinizing weather patterns and their impact on a predetermined parameter. For instance, in [104] the weather regimes were used to estimate Europe-wide wind power generation. Thus, the goal is to improve the drawbacks identified in the previous subsection by obtaining a forecast configuration for similar weather conditions. As related by several authors [94], the weather conditions have a strong impact on the wind power variability as well as in the uncertainty in its forecast. This can be partly explained by the weather conditions that unleash different responses, *e.g.*, heating and cooling between land/sea surfaces, and thermal stratification [57], [105], [106]. The performance of solar power forecast systems depends on the cloud coverage, which can be distinguished using weather regimes.

One of the objectives of this approach is to enable bidding strategically of market players by identifying the most adequate quantile (e.g., the quantile that maximizes the revenue in the day-ahead market) [107].

Below, further details of each step in the methodology implemented are provided:

- *Meteorological data*: The NWP data will be provided from the GFS global model. Several meteorological parameters from the NWP will be tested to identify meteorological features that enable to improve the wind or solar power forecast accuracy. New variables such as mean seal level gradient or atmospheric instability [57] to account for the energy conversion processes will be computed.
- *PCA analysis*: Before applying the principal components analysis (PCA) individually to each meteorological parameter, a z-score normalization process is applied. The normalization step ensures that the parameters in the dataset have comparable scales preventing to certain parameters dominating the principal components due to their larger magnitudes. The application of PCA helps identify the dominant spatial-temporal synoptic variability modes. In addition, by selecting a reduced number of

principal components (PC) poorly correlated local effects are removed. As a result, PCA reduces the dimensionality of the dataset [56]. In this study, PCA was individually applied to each meteorological parameter, and the number of retained (PCs) was determined based on the amount of variance they explain. The criterion used was to select the number of PCs that collectively account for 85% of the total variance [82].

- *Pearson coefficient correlation:* is then applied to identify the correlation between the PCs and the wind/solar PV power (or the combination of both) and the PCs are ranked in a descending way. In parallel with this process, a weather regime classification is computed.
- *Weather regime classification - clustering*: each forecast day will be classified into a specific WR using a clustering technique [108]. Clustering, an unsupervised learning technique, enables to unveil inherent patterns within data, grouping similar items without *prior* labelled guidance or supervision. The technique chosen was k-means, which is one the most used and well-known clustering algorithms due to its simplicity and easily interpretability easiness [109]. The k-means algorithm was applied in two slightly different ways, depending on whether dealing with aggregated (national) power data or power from a specific wind power plant. In the last case, it was considered hourly forecast meteorological data extracted for the specific wind power plant location. The clustering is based on three meteorological parameter – solar radiation and meridional and zonal wind components. It should be noted that these variables were normalized beforehand, using z-scores. For the aggregated case, k-means was conducted using the PCs from the variables. The points employed correspond to the meteorological grid locations within the respective country. The optimal number of clusters was determined through silhouette analysis [110]. However, this approach was constrained to a maximum of five clusters preventing the formation of imbalanced clusters, namely, clusters containing very few elements. This logic was founded on the principle of achieving specialized forecasts for distinct weather conditions. Consequently, all clusters need to comprise a significant number of elements.
- *FSS for each weather regime*: A greedy algorithm chooses the “most attractive” solution in each iteration. In this case, the SFS attempts to find the “optimal” feature subset by selecting, iteratively, the meteorological PC that reduces the RMSE value. Sensitivity tests will be implemented for each case study and technology to identify the most adequate objective function (OF). The OF will depend on the perspective: i) for market players as wind and solar power producers (or vRES aggregator), the RMSE and electricity market revenue (including day-ahead and imbalances) will be tested and compared, and ii) for the TSOs, the RMSE will be used. Some of most advanced statistical approaches Random Forest, Support Vector Machines (SVM), Extreme Gradient Boosting (XGBoost) and LightGBM are implemented.

The power forecast approach will be tested in the regional case studies defined in WP 5 where, the benefit from this approach from an electricity market will be further discussed as an outcome of WP 5.

4.1.2. TradeRES observed-based model forecast approach

Wind and solar forecasts of the minutes and hours ahead are nowadays a reality and they are used by power system operators to manage the balance of supply and demand,

or even in some electricity market products and a literature review of these models used can be found, for instance, in [15], [111]. In the TradeRES project different models based only on historical data (ML and traditional time series models like ARIMA), were utilized. For this type of power forecast, the historical power series was iteratively incorporated, encompassing power from the last hour up to the previous 24 hours and additionally, power from multiples of 24 hours up to a week was considered: $power_{h-1}$, $power_{h-2}$, ..., $power_{h-i}$, ..., $i = 3, ..., 24, 24*k, k= 2, ... 7$ (*i.e.*, starting from 24 hours, use multiples of 24 up to a week).

4.1.3. Deterministic power forecast models applied in the TradeRES project

Different models were designed to explore the time synergies and electricity market designs and their effectiveness in forecasting vRES outcomes across different time forecast horizons and case studies/regions within the scope of TradeRES. The different models analysed are:

1. NWP-based model
    - Employing NWP data and TradeRES methodology.

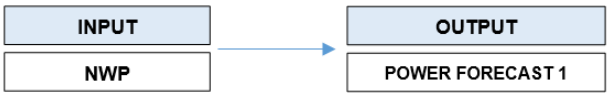

2. Power–based model
    - Black-box model using only power information from the historical power series.

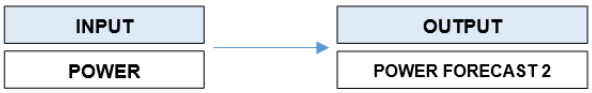

3. Hybrid model
    - Combination of the previous two models - incorporating a standard forecast (or raw NWP) and historical power series data.

In this deliverable, these models were applied for forecasting i) the next day comprising the 24-hour block, as required in the DAM, and ii) the next 6 hours, as required in the new market designs under analysis in the project. To effectively evaluate the best model for different market designs, a detailed analysis of various case studies is presented in section 5.

The output from this type of power forecast and the market players that can take advantage can be summarised as follows:

Output: Wind or solar power deterministic forecast with 60-minutes time resolution, according to the needs of the different players. When probabilistic forecasts are required, a quantile spline regression technique will be applied to obtain the probabilistic forecasts [106].

Market players that will benefit from these data: Wind and solar power producers, aggregators/virtual or hybrid power plants, and TSO.

4.2 Wind power ramping forecast

As the share of wind and solar PV increases in most of the power systems, ramping alert tools are being implemented by some TSOs [8], [113]. The goal of such tool is to complement the existing deterministic or probabilistic forecast systems enabling to increase the level of situational awareness available to the TSO by helping them to better scale the level of risk that exists in the system. This risk can then be managed by taking into consideration additional factors, such as potential changes in energy consumption, additional reserves that can be deployed, and additional generators that may be available for unit commitment. Furthermore, players capable to provide temporal and sectoral flexibility can also take advantage of this information to strategically participate into electricity markets.

The characterization and definition of wind power ramps are linked to the notion of an "*event that is critical enough to deserve special attention*" [60]. In specific, ramp events consist of a rapid and substantial change in the wind power during a time interval Δt. Since no clear definition is available in the literature to classify power ramps, the definition (15) and principles used in [10] will be followed in TradeRES project as a "first-guess".

$$\frac{\|Power(t+\Delta t)-Power(t)\|}{\Delta t} \geq PRRval \quad (15)$$

where, t denotes the time and $PRRval$ is the reference value. For these parameters, the values identified in [10] will be used.

Understanding power ramps events is not an easy task as the weather conditions are rarely the same for different wind parks. In fact, even when two wind parks are placed in similar latitudes, these triggering mechanisms can be very different due to local effects as the terrain characteristics, roughness and topography or phenomena like sea/land breezes [84]. Recent works, e.g., [10] state that, in order to understand and forecast the dynamics of wind power ramps, holistic methodologies should be used to account for the spatial and temporal evolution of atmospheric large-scale circulation. In this sense, in their work, the authors implemented a windstorm detection algorithm and compared the performance with a common cyclone detection algorithm [114], [115]. Windstorm algorithm presented a highest performance. Nevertheless, some issues were identified in the current windstorm detection methodologies. The most critical one is that a wind power ramp is not always a consequence or is always linked to the existence of extreme wind speed values, being essentially dependent from the previous (historical) state of the flow. Moreover, these algorithms are unable to distinguish upward from downward power ramps. For that reason, information from the previous time step ("memory effect") needs to be included in this type

of fast ramping tool. Therefore, this algorithm uses a time numerical differentiation in order to fit the particular case of wind power ramps events as described in the following subsections.

4.2.1. Ramp detection algorithm

This algorithm is based on the forecast mean sea level pressure from the NWP. In order to be able to identify areas where there is the highest variation in the meteorological field, the pressure gradient was calculated as follows:

$$\nabla P = \frac{\partial P}{\partial Long}\hat{\imath} + \frac{\partial P}{\partial Lat}\hat{\jmath} \approx \frac{P_{i+1,j} - P_{i-1,j}}{2\Delta Long} + \frac{P_{i,j+1} - P_{i,j-1}}{2\Delta Lat} \quad (16)$$

where *P* is the average pressure at sea level, *Long* the longitude and *Lat* the latitude. Next, and in order to introduce a "memory effect", the derivative in time of the pressure gradient is calculated according to the following expression:

$$\frac{\partial \|\nabla P\|}{\partial t} \approx \frac{\|\nabla P\|_t - \|\nabla P\|_{t-1}}{\Delta t} \quad (17)$$

The remaining detection algorithm is equal to the windstorm algorithm presented in [10]. Therefore, the major differences between the two methodologies are the following aspects: *i)* use of pressure data, ensuring better identification of the synoptic centres [10]; *ii)* identification of extreme events associated with positive/negative power changes in time, enabling a better relationship with the wind power ramp events. In this sense, it is considered that the events with negative variations are those with a change in the pressure gradient of less than the 2nd percentile. On the other hand, the positive events are identified as regions with a variation above the 98th percentile in the pressure gradient.

In the case of upward ramps, the algorithm starts to determine the grid points where the pressure gradient is above a certain percentile. The spatial percentile calculation is based on the following formula [10]:

$$\mathrm{Perc_x} = \mathrm{F_*^{-1}}(p) = \min\{\nabla \mathrm{P}: p \leq \mathrm{F_*}(\nabla \mathrm{P})\} \quad (18)$$

where, *p* represents the percentile considered and $\mathrm{F_*}$ stands for the cumulative distribution function weighted by the cosine of the latitude of {*W (Long, Lat, t):(Long, Lat)*$\in$δ} being δ the spatial domain [116]. For downward power ramps, the 2nd percentile is considered, and the search is for grid points where the pressure gradient is below this value.

Then, contiguous grid points for which the percentile condition occurs are enclosed into the same candidate [10]. A convex hull approximation is employed in this step to identify the convex polygon comprising all the spatial grid points that can belong to the same meteorological event (see black line in Figure 21). After, the average geometric center of each event is computed (magenta "*" symbols in Figure 21). As outcome, this spatial search algorithm provides a list of the possible location of events associated with synoptic systems. Only events with a minimum area of 150 000 km^2 [117] are considered. This step is performed for each temporal time-step.

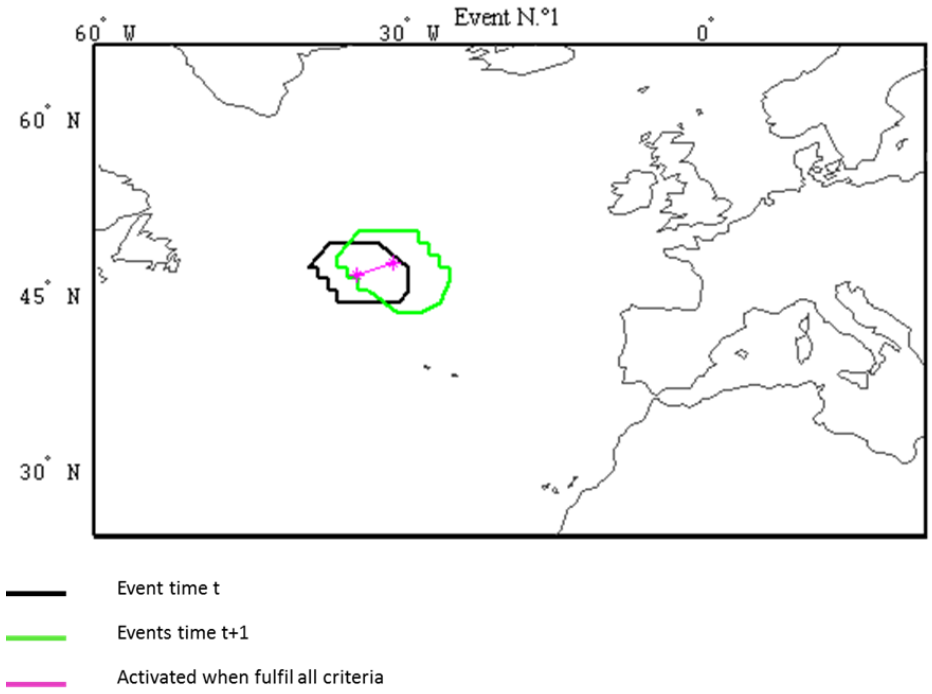

Figure 21. Example of one event in time *t* (black line) and one event in time *t+1* (green line). The magenta "*" symbols represent the average geometric center of each candidate, while the magenta line indicates the trajectory of the meteorological event.

Once the synoptic events are identified in the time step *t*, it becomes necessary to stitch to the nearest candidate at the time *t+1* to build the trajectory. The following assumptions are imposed in this step [10]:

1. The maximum Euclidean distance between the centers of two consecutive time-steps is 720 km [117];
2. Only events with a lifetime above 2h or with a maximum speed of 120 km/h are retained.

All events with no continuity are eliminated, and when two or more candidates are found, a cost function is applied in order to determine the most appropriate trajectory. The cost function applied is similar to the one shown by [118], which is expressed by:

$$\text{Tracking} = \text{argmin}\left(\sum_{j=1}^{j=N}(C_t - C_{t+1,j}) \times \left(\left\|\frac{Int_t - Int_{t+1,j}}{Int_t}\right\|\right)\right) \quad (19)$$

where, C_t are the coordinates of the center for a determined synoptic event at time step *t*, $C_{t+1,j}$ are the coordinates of the center for the *j*th synoptic event at time step t+1, Int_t is the intensity observed at the geometric center of the event at time-step *t* and $Int_{t+1,j}$ is the intensity observed of the geometric center for the *j*th synoptic event at time-step *t+1*.

At the end, the algorithm retains a tracking table with the different trajectories of the extreme events detected and some basic characteristics, *e.g.*, their lifetime, occurrence dates, speed, area of influence. In real-time operation, an alert will be issued when these events are nearby the region under analysis.

The power ramp power forecast accuracy will be assessed and analysed in the regional cases from WP 5.

4.2.2. A nested forecast approach

Based on the probabilistic and power ramp detection algorithm, a nested forecast approach will be established aiming to reduce the system cost associated with less committed reserves. Thus, the power reserves' allocation can be dynamically established and dependent on the probability of existence (or not) of wind ramps. Other market players as flexibility providers or wind power producers can also benefit from this nested approach since it can allow for strategic participation in electricity markets. An example of the outcomes of this tool is shown in Figure 22.

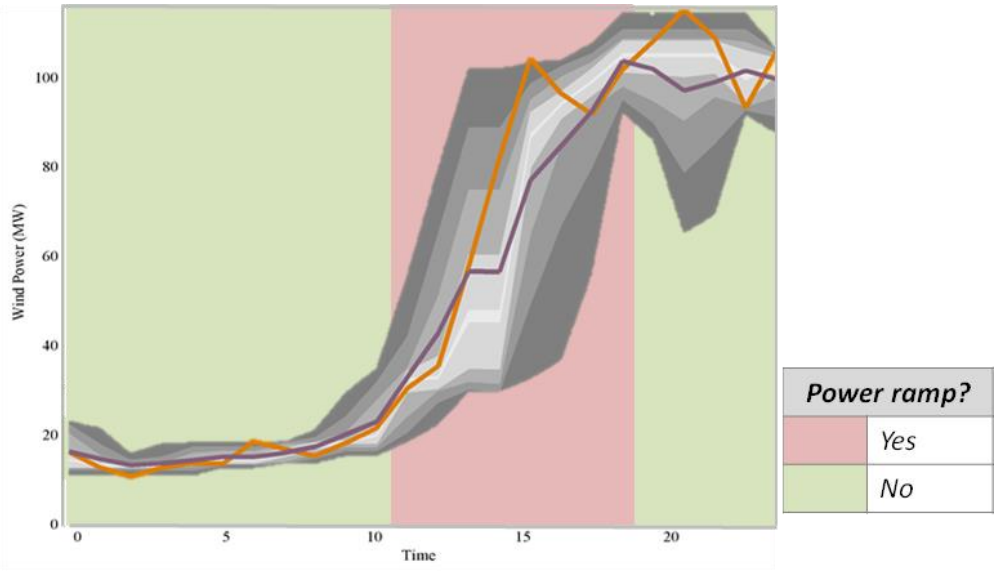

Figure 22. Example of the outcomes from the nested forecast approach. Green regions: no power ramp is expected; Red regions: a power ramp is expected

The output from this type of power forecast and the market players that can take advantage can be summarised as follows:

Output: Hourly binary information regarding the occurrence (or not) of wind power ramps.

Market players that will benefit from these data: All TradeRES agent-based models may benefit from these data by incorporating it in TSO agent capabilities or in flexibility provider and wind power producers' agent behaviour, using this information to strategically participate in the electricity markets.

5. Application of the forecast approaches developed in TradeRES

Simulations involved forecasting wind and solar power in Portugal, Spain, and Germany, covering 27 wind parks and 8 solar PV parks in Portugal. The 27 wind parks have nominal powers ranging from 17 MW to 255 MW (average of 68 MW) and are distributed throughout continental Portugal, with a higher density in the North and Centre of the country. The 9 solar parks have nominal powers ranging from 8 MW to 40 MW (average of 17 MW) and are mainly located in the South of Portugal. For the national cases, data from Ninja.Renewables (extracted from https://www.renewables.ninja – see more details at [119]) were used as target, while the target variable for each Portuguese wind power plant was the observed hourly power production. Simulations were performed considering the: i) 24-hour period forecast needed for the DAM, using the existing and new gate closure hours (section 5.2); ii) alternative electricity market design – PAM which requires updated forecasts at 00:00, 06:00, 12:00, and 18:00 (section 5.3). Three forecasting scenarios were simulated across Portugal, Spain, and Germany exploring NWP-based models and the potential of incorporating real-time data from power production. Predictive models were trained using data from 2018 and then tested on the entire dataset from 2019.

5.1 Case studies, data and vRES forecasting models

For the **NWP-based model** the methodology described in section 4.1.1 was employed, incorporating slight modifications to explore different testing conditions. The changes and adaptations to the methodology are briefly described next. Meteorological data was derived directly from GFS. The data were collected from a grid of points spanning Portugal, Germany, and Spain, ensuring a comprehensive analysis of meteorological conditions across these countries, Figure 23.

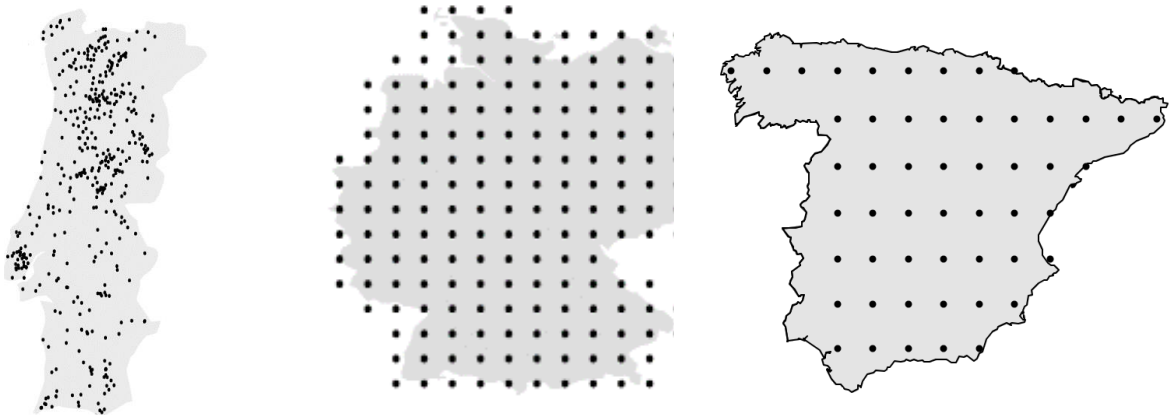

Figure 23. Points extracted from the NWP for the different case studies: Portugal, Germany, and Spain.

As shown in Figure 23, the grid of meteorological points across Portugal is not regular in order to take advantage of the meteorological data availability from the Portuguese forecast provider, Smartwatt (now Enlitia). For Germany, it was considered a regular grid over Germany as presented in Figure 23 as well as for Spain.

For the aforementioned case studies, the same weather variables were considered:

- Wind speed (at 10m, 50m and 100m)
- Wind gust (at 10m)
- Wind direction (at 10m, 50 m and 100m)
- Temperature (2m, 80 m)
- Mean sea level pressure
- Solar irradiance at surface
- Relative humidity (2m)
- Geopotential height (at 500, 850 hPa)
- Planetary boundary layer height

Following the collection of meteorological data, Principal Component Analysis (PCA) was applied to each meteorological indicator in the training dataset after standardization. It is essential to highlight that a separate standardization and PCA process was not conducted for the test dataset. Instead, the transformation applied to the training data was directly employed for the test dataset. The criteria for selecting principal components involved retaining those collectively explaining over 85% of the variance. The resulting components were utilized as features. Alongside, to identify typical days or weather patterns, k-means clustering was employed using hourly values of wind u and v components and radiation throughout the training period. In the case study of Portuguese wind power plants, k-means was applied individually to each wind power plant, considering the specific location's meteorological indicators. On a global scale, this was done considering the principal components retained for these meteorological indicators. The optimal number of clusters was determined based on inertia values. Like PCA, clustering was applied to the training dataset, and for each unseen data point in the test dataset, predicting the respective cluster involved calculating the Euclidean distance between the data point and the cluster centroids.

Various forecasting models were tested, considering two scenarios - with and without clustering. This encompassed testing different features (resulting from PCA) and various regression algorithms. In both case studies, Lasso Regression was utilized for feature selection due to its performance. In the clustering scenario, feature selection and algorithm testing were conducted for each cluster.

The regression algorithms examined included Random Forest, Support Vector Machine, LightGBM, and XGBoost. Initially, these algorithms were tested with default hyperparameters and subsequently fine-tuned for enhanced performance. The final choice was LightGBM, primarily for its speed advantage and superior performance, as evidenced by the Table 5 comparing it to other standard machine learning algorithms. The results in the table refer to simulations for the national total of wind (renewables ninja) for the PAM horizon. The LightGBM algorithm underwent training on 2018 data, and it was used to predict the entire year of 2019.

Table 5. Wind power NRMSE values for different ML methods using Portugal as a case study.

ML technique	NRMSE (%)		
	Portugal	Germany	Spain
LightGBM	24.10	20.20	18.38
Gradient Boosting regression	25.06	20.49	18.38
XGBoost	25.71	23.26	19.49
SVM	28.33	39.99	23.99
Random Forest	25.46	21.79	18.43

For the **model based only on historical data (*power-based model*)**, different regression techniques, including traditional time series models like ARIMA, were utilized (more details are available in section 4.1.2). Ultimately, to maintain consistency and based on the results, LightGBM was employed.

For the **hybrid approach** (more details available in section 4.1.3) it was applied the NWP data**,** represented by the principal components retained for the meteorological indicators, and data from the historical power series, also including different lags ranging from the previous hour up to a week.

5.2 Simulation results for day ahead market with new gate closure

Table 6 presents the results for Portugal and Spain using updated initial and boundary conditions, assuming a postpone of the gate closure of the day-ahead market, as depicted in Figure 10. These forecasts are only based on NWP data.

Table 6. Wind and solar power NRMSE (%) for DAM according to different IBCs for 2019.

IBC hour from	Wind		Solar	
	Portugal	Spain	Portugal	Spain
6 UTC	29.51	20.22	28.32	20.73
12 UTC	28.55	21.80	32.69	20.53
18 UTC	26.28	19.54	28.51	20.99

The findings presented in Table 6 indicate that the impact of incorporating updated initial boundary conditions on forecast certainty is not significant in the case studies analysed. In certain instances, the utilization of refreshed forecasts may even lead to inferior performance. These results can be partially explained using power forecasts that use different features to improve their performance according to each IBC condition. In addition, as discussed in [120] despite assimilating a comparable number of observations for IBC generation in the global NWP models, the different sources of these data (such as weather stations, land soundings, aircraft, and satellites) exhibit significant variations throughout

the day. This variability can introduce complexities into the final results. Additionally, the different cycles coincide with periods of increased atmospheric instability in Portugal and Spain due to the sunrise/sunset of the Sun or transition between different weather regimes, making it more challenging for the model to accurately predict future states of the atmosphere. Therefore, the results suggest that the benefits of using new updated IBC are not always straightforward and should be carefully analysed.

5.3 Comparison of power forecast results for the day and period ahead markets

The subsequent section will specifically detail studies focusing on forecasts for the day ahead at 12:00 (as required in DAM) and the four daily updates at 00:00, 06:00, 12:00, and 18:00 (as required in PAM), as schematic represented in Figure 11.

5.3.1. Wind power

The results, in Table 7, show that the hybrid model result is advantageous for the four updates, but also for day ahead forecast in the case of wind power. The power-based model has a very poor performance for the day-ahead market period. Figure 24 presents the NRMSE for the wind parks using the different methods.

Table 7. Wind power forecast results for day and period ahead markets (SD refers to standard deviation of the results for all wind parks).

Market design	Simulation	Portugal	Germany	Spain	Wind Parks
DAM	Historical Power	70.50	73.19	51.78	98.50 (SD = 5.19)
	Historical Power + NWP	**31.16**	23.72	**21.29**	**66.52** (SD = 7.97)
	NWP	31.86	**21.67**	21.79	71.78 (SD =11.68)
PAM	Historical Power	24.70	28.75	20.37	57.59 (SD = 6.29)
	Historical Power + NWP	**21.99**	**18.04**	**13.39**	**51.64 (SD =5.35)**
	NWP	24.02	20.10	18.15	60.92 (SD =4.98)

Figure 24 depicts the results obtained in the simulations of different models for the 27 wind parks for DAM and PAM, respectively. Figure 24a) shows that, in general, the hybrid model based on NWP and historical power series tends to have better performance than the NWP-based model, although the results are sometimes very similar. The power-based model is clearly the least favorable. Figure 24b) allows us to observe the advantage of including data from the historical power series combined with meteorological variables.

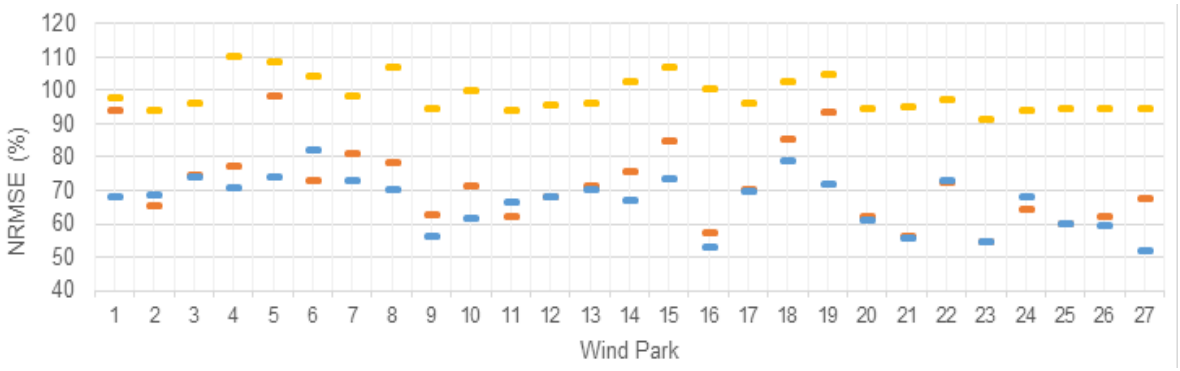

a) Forecasts for DAM.

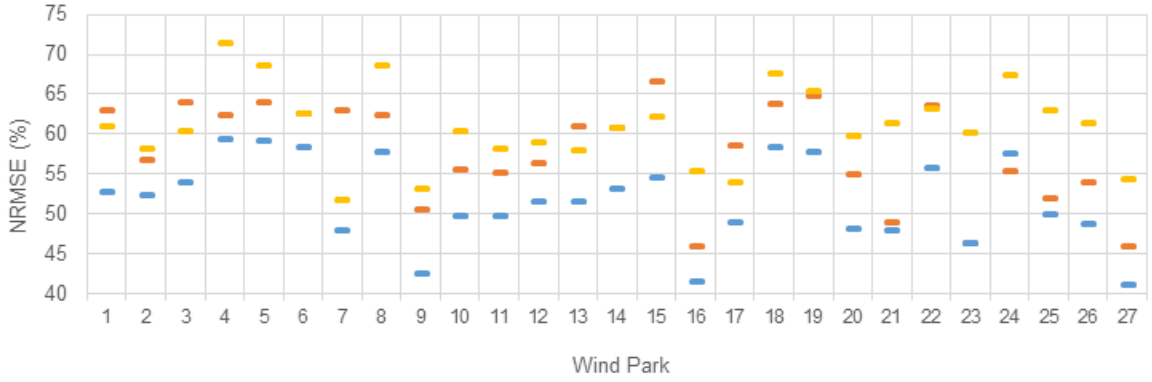

b) Forecasts for PAM.

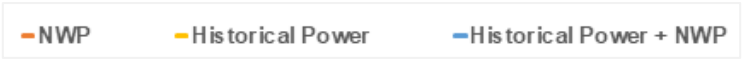

Figure 24. Wind power NRMSE for the different wind power parks analysed in Portugal considering the a) DAM and b) PAM timeframes.

The following graphs (Figure 25 and Figure 26) show the total wind national Portuguese power forecasts for different months. For the existing DAM design, the forecast based solely on the historical series performs poorly when compared to the NWP-based model and the hybrid model. In the case of updates for the next 6 hours every four hours, the performance is better, being even very close to the NWP-based model.

The significance of specific lags in forecasting depends on whether the focus is on a national or park level. During the simulations, it was observed that the significance of specific lags from the power series depended on whether the focus was national or at the park level. For example, at the park level, the importance of variables related to lags of 3 or more days was noticeable. Additionally, the results for the Portuguese case revealed lower performance when compared to Spain and Germany. This can be partially attributed to the lower installed wind power capacity, which reduces the potential benefit from the power smoothing effect to improve the forecast accuracy [77], [78].

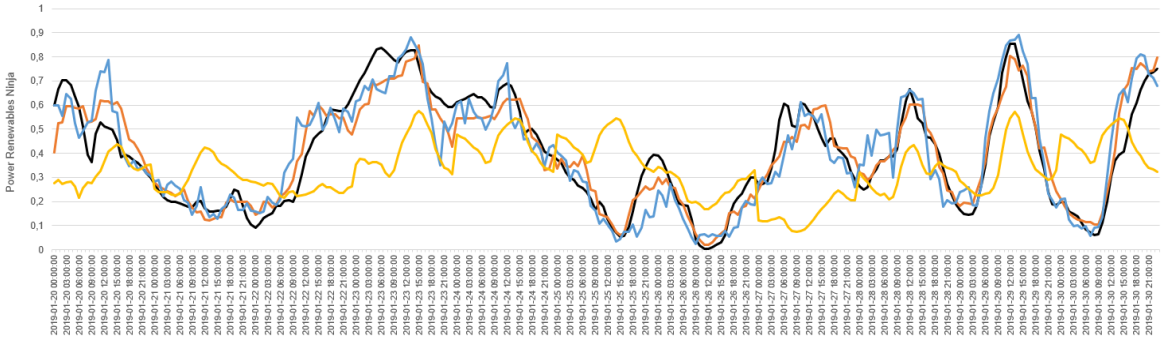

a) Forecasts for DAM – Results for 10 days of Winter 2019 (20th to 30th January).

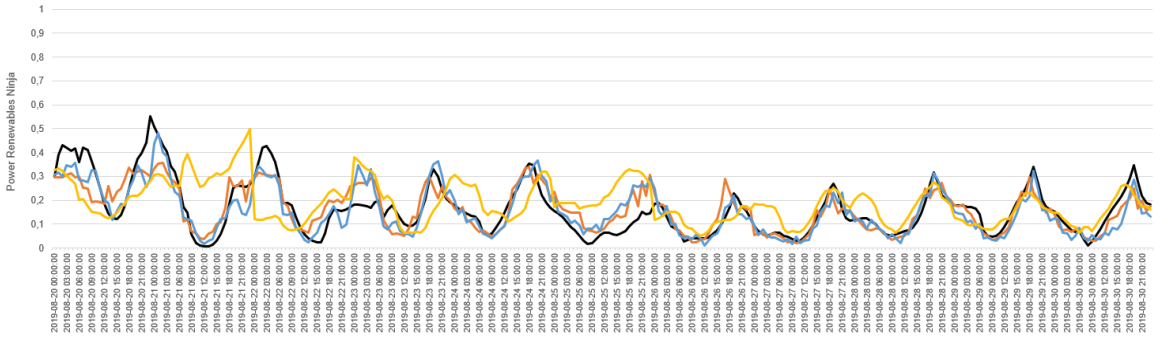

b) Forecasts for DAM - results for 10 days of Summer 2019 (20th to 30th August).

Figure 25. Portuguese aggregated wind power forecast considering the DAM design for some days in the a) Winter and b) Summer period of 2019.

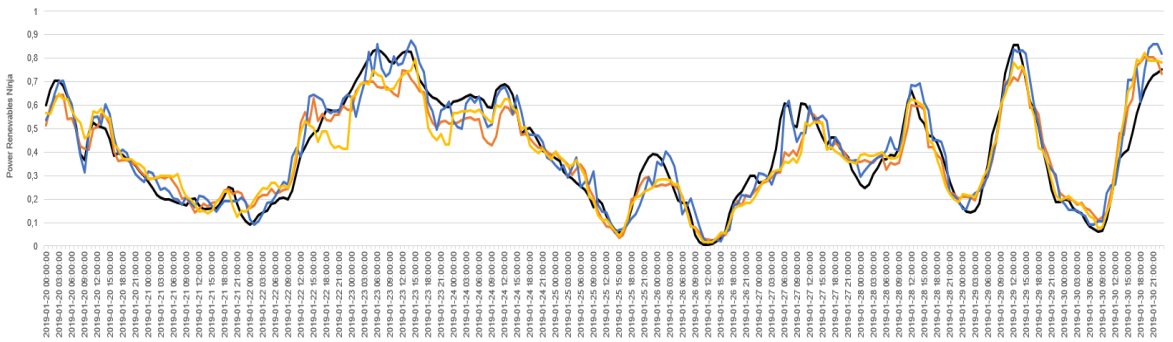

a) Forecasts for PAM – Results for 10 days of Winter 2019 (20th to 30th January).

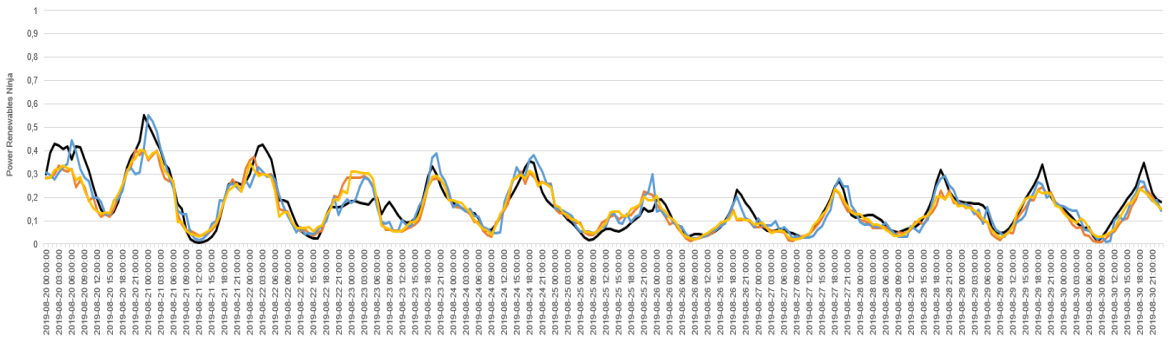

b) Forecasts for PAM - results for 10 days of Summer 2019 (20th to 30th August).

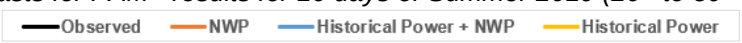

Figure 26. Portuguese aggregated wind power forecast considering the PAM design for some days in the a) Winter and b) Summer period of 2019.

Furthermore, the performance of different models was analysed for a short-term horizon (Figure 27). In addition to the models that have been considered, a persistence model was also included, consisting of maintaining the value of power for the initial forecast hour. This analysis was conducted for each of the case studies and for the 27 wind parks. The behaviour in the three national cases is very similar. The persistence model exhibits the best performance up to the next two hours. The NWP-based model shows nearly constant error behaviour. The hybrid model (NWP + Historical power) outperforms the NWP model in the first four hours (Germany and Spain), after which they become very analogous in terms of error. The model based solely on power also experiences a degradation in performance as the time horizon increases, while maintaining the power value.

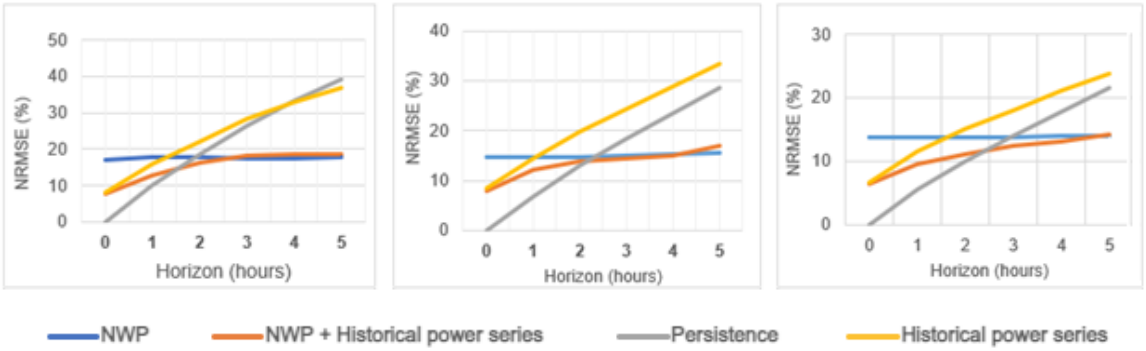

Figure 27. Comparison of different short-term horizon models (left: Portuguese case study, center: Germany, right: Spain).

In Figure 28, the comparison of NRMSE for various short-term forecast time horizons (in hours) and models across the 27 wind parks under analysis is illustrated using a box plot. This graphical representation highlights the statistical distribution of NRMSE for different horizons. Within the box plot, a red mark at the centre denotes the median, and the box spans from the 25th to the 75th percentiles. The whiskers extend up to 1.5 times the interquartile range, signifying the data's dispersion. Outliers are visually indicated as black diamonds.

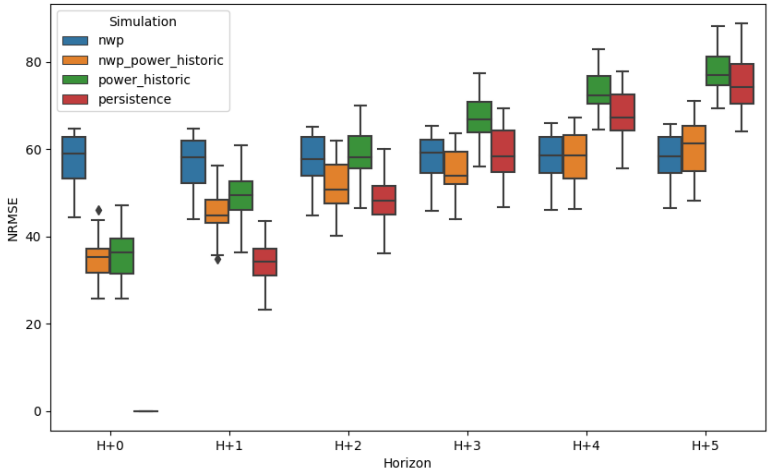

Figure 28. Comparison of NRMSE (%) for different short-term forecast time horizons (in hours) and models for the 27 wind parks under analysis.

Similarly, for the 27 wind parks, the logic is analogous. The persistence error progressively increases with the time horizon, as does the error of the model based on historical power series. As the horizon extends, the hybrid model slightly degrades in performance, becoming then similar to the NWP-based model. A similar behaviour is observed for two wind parks, event with distinct performance levels, Figure 29.

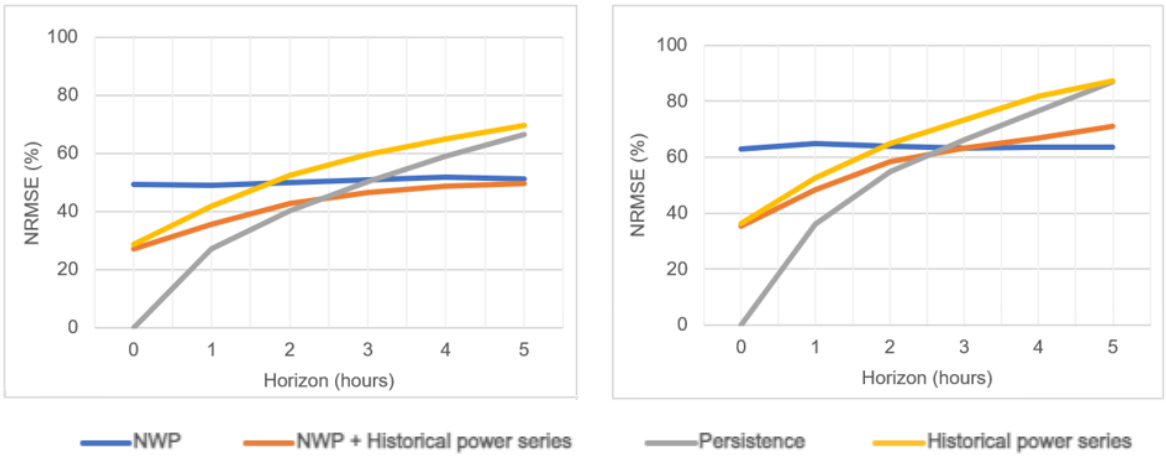

Figure 29. Detailed analysis of NRMSE (%) for two specific wind parks and for different short-term forecast time horizons (in hours).

Also, for the wind power plants tested, using the TradeRES NWP-based model, it was observed an average decrease of 5.47% in NRMSE (standard deviation 2.8%) and a maximum decrease of 10.13%, when compared to the operational NWP-based model of the provider for the same data source.

5.3.2. Solar power

The simulations carried out for the wind case were also conducted for the solar case. Table 8 presents the obtained results.

Table 8. Solar PV power forecast results for day and period ahead markets.

Market design	Simulation	Portugal	Germany	Spain	Solar Parks
DAM	Historical Power	34.98	46.74	25.07	60.53 (SD = 2.37)
	Historical Power + NWP	**24.85**	**34.89**	**19.97**	**50.34 (SD = 2.19)**
	NWP	32.69	30.99	20.53	58.21 (SD = 3.26)
PAM	Historical Power	24.29	33.41	17.85	52.75 (SD = 1.97)
	Historical Power + NWP	**19.16**	**29.56**	**15.64**	**47.23** (SD = 2.07)
	NWP	27.82	30.69	20.61	52.58 (SD = 1.91)

The outcomes align with those obtained for the wind power case. The results, in Table 8, show that the hybrid model result advantageous for the four updates, but also for day ahead forecast in the case of solar power. The power-based model has a very poor per-

formance for day ahead. Figure 30 presents the NRMSE for the wind parks using the different methods.

The graphs presented in Figure 30a) and b) illustrate the outcomes derived from simulations using various models for the parks under the scenarios of DAM and PAM, respectively. For the 8 solar parks, even in the PAM scenario, significant errors are observed. However, in all cases, the combination of NWP and power history helps reduce the error compared to other models.

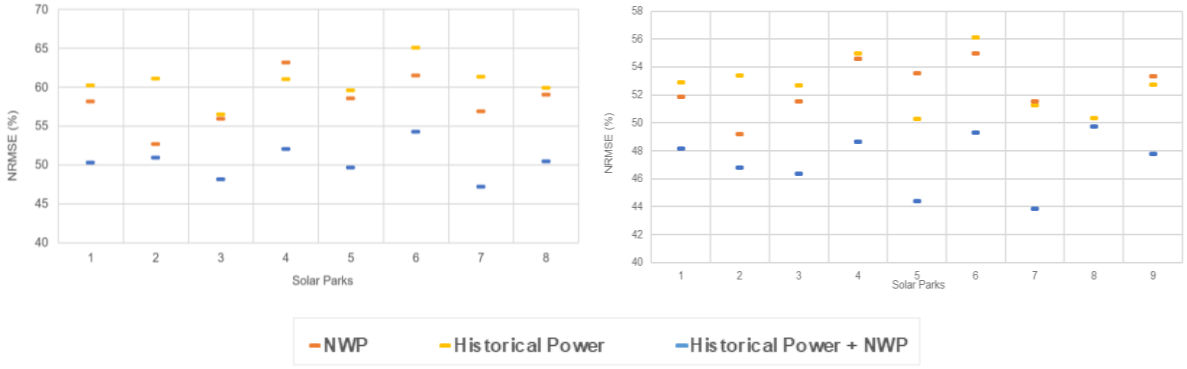

Figure 30. Solar power NRMSE for the different solar power parks analysed in Portugal considering the a) DAM and b) PAM timeframes.

Figure 31 and Figure 32 show the total national Spanish solar power forecasts for different months.

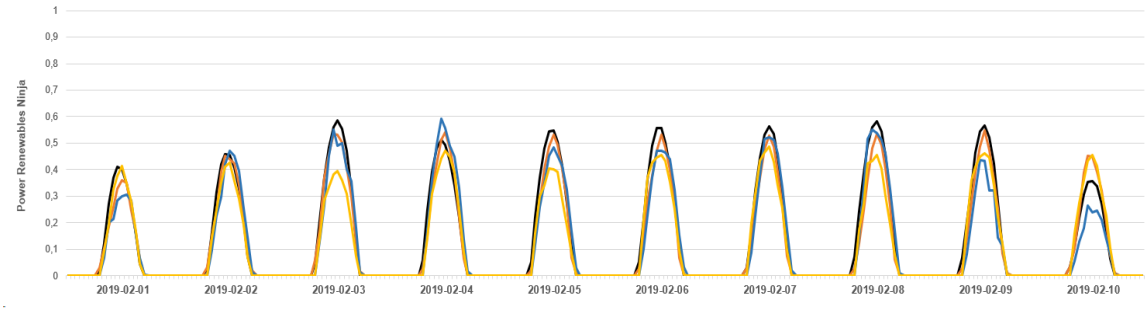

a) Forecasts for DAM – Results for 10 days of Winter 2019 (01st to 10th February)

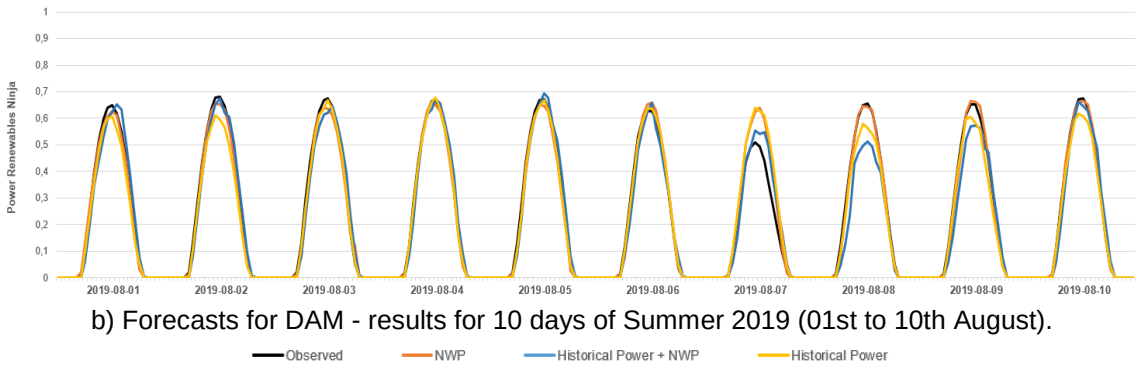

b) Forecasts for DAM - results for 10 days of Summer 2019 (01st to 10th August).

Figure 31. Spanish aggregated solar power forecast considering the DAM design for some days in a) Winter and b) Summer period of 2019.

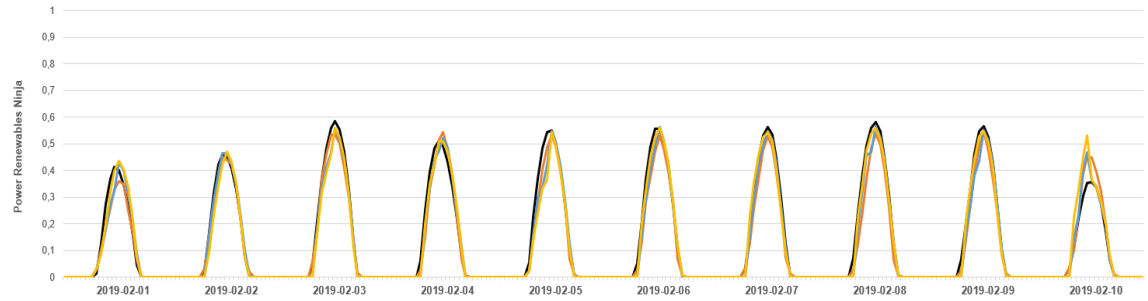

a) Forecasts for PAM – Results for 10 days of Winter 2019 (01st to 10th February)

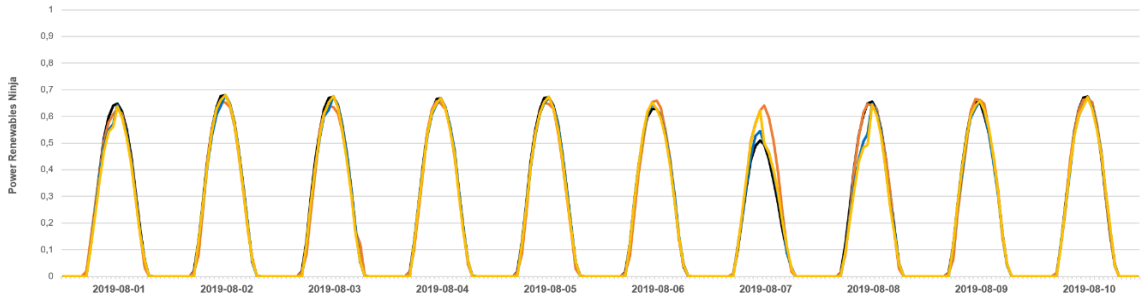

b) Forecasts for PAM - results for 10 days of Summer 2019 (01st to 10th August)

Figure 32. Spanish aggregated solar power forecast considering the PAM design for some days in a) Winter and b) Summer period of 2019.

Figure 31 shows that for DAM in solar power, the performance of the model based on the historical power series is not as poor as observed for wind power. It also shows that in the winter months, a) the performance tends to be worse compared to the summer months, where there are more consecutive clear sky days. Figure 32b) particularly suggests the importance of the combination between NWP and historical power data. Furthermore, the performance according to the different forecast time horizons and models was also analysed for the solar power case. In addition to the models that have been considered, a persistence model was also included, consisting of maintaining the value of power for the initial forecast hour. This analysis was conducted for each national case study (Figure 33) and for 8 solar parks (Figure 34).

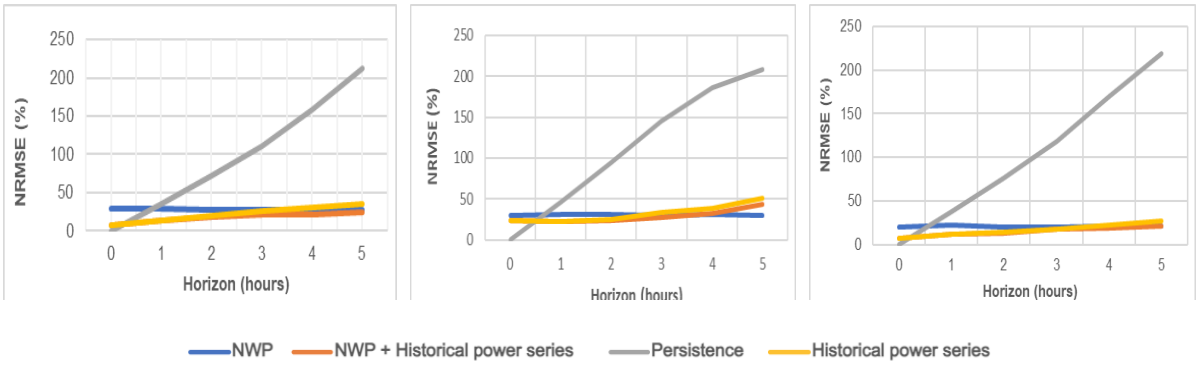

Figure 33. Comparison of different short-term horizon models for solar power forecast (left: Portuguese case study, centre: Germany, right: Spain).

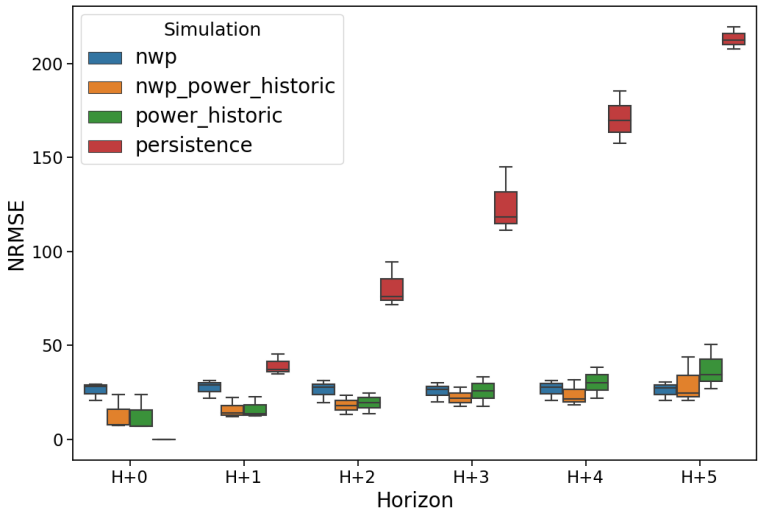

Figure 34. Comparison of NRMSE (%) for different short-term forecast time horizons (in hours) and models for the 8 solar parks under analysis.

As observed in the wind power model, errors increase as the forecasting horizon extends. However, in this case, the persistence model error exhibits a significant increase, even for 1-hour ahead forecast. The performance of the hybrid model shows a slight decline with a longer horizon, eventually reaching a level comparable to that of the NWP-based model.

For solar parks, a similar trend to the national scenario is observed in the boxplots illustrating the NRMSE distribution, as depicted in Figure 34 across various time horizons. As the forecasting horizon increases, the performance of the persistence model degrades significantly. The model based on historical power series also shows a tendency to degrade its performance. Meanwhile, the NWP model error remains relatively stable throughout the horizons considered. The hybrid model tends to degrade its performance, although to a lesser extent, and remains somewhat comparable, though inferior, to the NWP model. Details for two specific solar parks are provided in Figure 35.

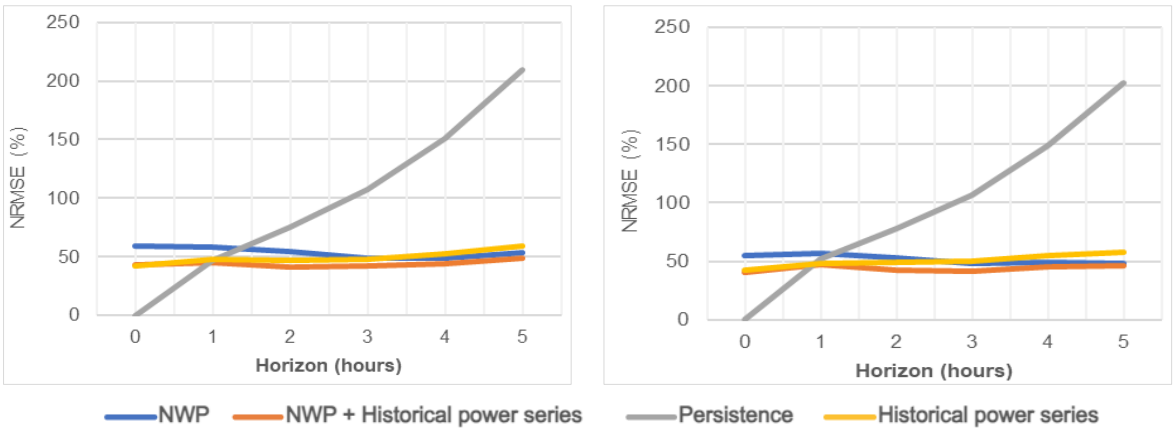

Figure 35. Detailed analysis of NRMSE (%) for two specific solar parks and for different short-term forecast time horizons (in hours).

6. Final remarks

In this report, a non-extensive review of the different forecasting methods was presented focusing on the variable renewable energy systems (vRES) under analysis in the TradeRES project. This review served as the basis for framing the advantages and disadvantages of the different forecast approaches commonly applied in the energy sector. Moreover, it allowed to identify the synergies among the different approaches and existing electricity market time-frames. Based on this background different forecasting methods were developed to be used in the TradeRES project.

To improve the existing forecast systems, a new numerical weather (NWP)-based approach is proposed in TradeRES. Different models, various technologies, and multiple forecast horizon scenarios were tested, considering only NWP, historical power series, or their combination. The findings indicated that employing a grid of meteorological points yields superior performance compared to relying on a single meteorological point for forecasting, outperforming the operational model of Enlitia based on the same NWP global model used in TradeRES for a single meteorological point. Additionally, it was observed that incorporating non-conventional meteorological variables, such as the atmospheric boundary layer, is crucial for enhancing the accuracy of wind and solar power forecasts. The clustering process, used to identify typical weather patterns, also significantly contributes to performance improvement.

The results show that for both technologies the use of NWP had a clear impact on the forecast for the next 24 hours compared to the model based solely on the historical power series. On the other hand, the combination of NWP and the historical production series proved to be advantageous. Consequently, power producers should invest in enabling real-time access to observed power data by the forecast providers to enhance the accuracy of power forecasts. For the time-frame of the day-ahead market wind and solar PV technologies continue to show significant errors, even assuming a postponement of their bids to an hour closer to real-time. For the timeframes of the alternative market designs analysed in this deliverable (below six hours), NWP-based results show an inferior performance when compared with approaches that forecast future values based on past values.

Using the agent-based market model AMIRIS it was possible to demonstrate that realistic forecasts can significantly reduce the profits of operators of onshore wind producers in the German day-ahead market. This is due to the frequent occurrence of slight underestimates of wind power production in the underlying distribution of the forecast time series. Assuming Gaussian-distributed errors in wind power production, however, results in smaller losses. This finding highlights the importance of the forecast error distribution for market outcomes. Future research could aim to model more realistic forecast errors for different plant regions in Germany and quantify their impact on the overall market.

Finally, it should be highlighted that the work conducted in this T4.4, which is summarised in this report, paves the way for addressing specific market designs and product choices identified in TradeRES project. The detailed impact of these results on electricity markets will be presented in the forthcoming WP 5 deliverables, namely, in *D5.3 - Perfor-*

mance assessment of current and new market designs and trading mechanisms for National and Regional Markets.

The power forecast tools created as part of this task will be made accessible to the public via GitHub and disseminated using the dissemination channels established in the project. The goal is to ensure that users interested can have the capability to execute the tools and obtain power forecasts that can be used in future studies or as benchmarking.

References

[1] S. Hanifi, X. Liu, Z. Lin, and S. Lotfian, “A Critical Review of Wind Power Forecasting Methods—Past, Present and Future,” *Energies*, vol. 13, no. 15, p. 3764, Jul. 2020, doi: 10.3390/en13153764.

[2] C. Croonenbroeck and G. Stadtmann, “Renewable generation forecast studies – Review and good practice guidance,” *Renew. Sustain. Energy Rev.*, vol. 108, no. June 2018, pp. 312–322, Jul. 2019, doi: 10.1016/j.rser.2019.03.029.

[3] H. Holttinen *et al.*, “Methodologies to determine operating reserves due to increased wind power,” *IEEE Trans. Sustain. Energy*, vol. 3, no. 4, pp. 713–723, Oct. 2012, doi: 10.1109/TSTE.2012.2208207.

[4] H. Algarvio, A. Couto, F. Lopes, and A. Estanqueiro, “Changing the Day-Ahead Gate Closure to Wind Power Integration: A Simulation-Based Study,” *Energies*, vol. 12, no. 14, p. 2765, Jul. 2019, doi: 10.3390/en12142765.

[5] L. de Vries *et al.*, “D3.5 - Market design for a reliable ~ 100 % renewable electricity system,” *TradeRES project deliverable*. p. 62, 2021 [Online]. Available: https://traderes.eu/wp-content/uploads/2021/04/D3.5_MarketDesignOptions_H2020.pdf

[6] L. de Vries *et al.*, “D3.5 - Market design for a reliable ~ 100 % renewable electricity system (Ed. 2),” *TradeRES project deliverable*. p. 81, 2023.

[7] C. Köhler *et al.*, “Critical weather situations for renewable energies – Part B: Low stratus risk for solar power,” *Renew. Energy*, vol. 101, pp. 794–803, Feb. 2017, doi: 10.1016/j.renene.2016.09.002.

[8] A. Steiner *et al.*, “Critical weather situations for renewable energies – Part A: Cyclone detection for wind power,” *Renew. Energy*, vol. 101, pp. 41–50, Feb. 2017, doi: 10.1016/j.renene.2016.08.013.

[9] C. Gallego-Castillo, E. Garcia-Bustamante, A. Cuerva, and J. Navarro, “Identifying wind power ramp causes from multivariate datasets: a methodological proposal and its application to reanalysis data,” *IET Renew. Power Gener.*, vol. 9, no. 8, pp. 867–875, 2015, doi: 10.1049/iet-rpg.2014.0457.

[10] M. Lacerda, A. Couto, and A. Estanqueiro, “Wind Power Ramps Driven by Windstorms and Cyclones,” *Energies*, vol. 10, no. 10, p. 1475, Sep. 2017, doi: 10.3390/en10101475.

[11] M. S. H. Lipu *et al.*, “Artificial Intelligence Based Hybrid Forecasting Approaches for Wind Power Generation: Progress, Challenges and Prospects,” *IEEE Access*, vol. 9, pp. 102460–102489, 2021, doi: 10.1109/ACCESS.2021.3097102.

[12] J. Yan, C. Möhrlen, T. Göçmen, M. Kelly, A. Wessel, and G. Giebel, “Uncovering wind power forecasting uncertainty sources and their propagation through the whole modelling chain,” *Renew. Sustain. Energy Rev.*, vol. 165, p. 112519, Sep. 2022, doi: 10.1016/j.rser.2022.112519. [Online]. Available: https://linkinghub.elsevier.com/retrieve/pii/S1364032122004221

[13] D. Yang and D. van der Meer, “Post-processing in solar forecasting: Ten overarching thinking tools,” *Renew. Sustain. Energy Rev.*, vol. 140, no. 110735, p. 35, 2021, doi: 10.1016/j.rser.2021.110735. [Online]. Available: https://doi.org/10.1016/j.rser.2021.110735

[14] R. Ahmed, V. Sreeram, Y. Mishra, and M. D. Arif, “A review and evaluation of the state-of-the-art in PV solar power forecasting: Techniques and optimization,” *Renew. Sustain. Energy Rev.*, vol. 124, no. 109792, p. 26, May 2020, doi: 10.1016/j.rser.2020.109792. [Online]. Available: https://doi.org/10.1016/j.rser.2020.109792

[15] R. Tawn and J. Browell, “A review of very short-term wind and solar power forecasting,” *Renew. Sustain. Energy Rev.*, vol. 153, p. 111758, Jan. 2022, doi: 10.1016/j.rser.2021.111758. [Online]. Available: https://linkinghub.elsevier.com/retrieve/pii/S1364032121010285

[16] D. C. Montgomery, C. L. Jennings, and M. Kulahci, *Introduction to Time Series Analysis and*

Forecasting, 2nd ed. New Jersey: JohnWiley & Sons, Inc., 2015.

[17] C. Chatfield, *Time-Series Forecasting*. Florida: Chapman and Hall/CRC; 6th edition (July 31, 2003), 2000.

[18] C. Kuster, Y. Rezgui, and M. Mourshed, “Electrical load forecasting models: A critical systematic review,” *Sustain. Cities Soc.*, vol. 35, no. August, pp. 257–270, 2017, doi: 10.1016/j.scs.2017.08.009.

[19] Y. H. Hsiao, “Household Electricity Demand Forecast Based on Context Information and User Daily Schedule Analysis From Meter Data,” *IEEE Trans. Ind. Informatics*, vol. 11, no. 1, pp. 33–43, 2015, doi: 10.1109/TII.2014.2363584.

[20] B. Yang *et al.*, “State-of-the-art one-stop handbook on wind forecasting technologies: An overview of classifications, methodologies, and analysis,” *J. Clean. Prod.*, vol. 283, p. 124628, 2021, doi: 10.1016/j.jclepro.2020.124628.

[21] J. Widén, N. Carpman, V. Castellucci, D. Lingfors, J. Olauson, and et al., “Variability Assessment and Forecasting of Renewables: A Review for Solar, Wind, Wave and Tidal Resources,” *Renew. Sustain. energy Rev.*, vol. 44, pp. 356–375, 2015.

[22] C. Monteiro, R. Bessa, V. Miranda, A. Botterud, J. Wang, and G. Conzelmann, “Wind Power Forecasting: State-of-the-art 2009,” 2009 [Online]. Available: https://publications.anl.gov/anlpubs/2009/11/65613.pdf

[23] T. Haiden, M. . Janousek, F. . Vitart, Z. Ben-Bouallegue, and F. Prates, “Evaluation of ECMWF forecast, including 2023 upgrade,” *ECMWF Technical Memoranda 911*. p. 60, 2023 [Online]. Available: https://www.ecmwf.int/sites/default/files/elibrary/092023/81389-evaluation-of-ecmwf-forecasts-including-the-2023-upgrade.pdf

[24] C. Sweeney, R. J. Bessa, J. Browell, and P. Pinson, “The future of forecasting for renewable energy,” *WIREs Energy Environ.*, vol. 9, no. 2, Mar. 2020, doi: https://doi.org/10.1002/wene.365.

[25] Portal do Clima, “Portal do Clima - Climate Change in Portugal,” *Programa ADAPT Alterações Climáticas em Portugal*, 2021. [Online]. Available: http://portaldoclima.pt/en/project/methodology/climate-models/. [Accessed: 01-Sep-2021]

[26] A. Couto, L. Rodrigues, P. Costa, J. Silva, and A. Estanqueiro, “Wind power participation in electricity markets - The role of wind power forecasts,” in *EEEIC 2016 - International Conference on Environment and Electrical Engineering*, 2016, p. 6, doi: 10.1109/EEEIC.2016.7555453.

[27] R. Lam *et al.*, “Learning skillful medium-range global weather forecasting,” *Science (80-.).*, vol. 382, no. 6677, pp. 1416–1421, Dec. 2023, doi: 10.1126/science.adi2336. [Online]. Available: https://www.science.org/doi/10.1126/science.adi2336

[28] R. Marujo, P. Costa, M. Fernandes, T. Simoes, and A. Estanqueiro, “Offshore wind field: Application of statistical models as a spatial validation technique,” in *European Offshore Wind Conference & Exhibition*, 2011, p. 8 [Online]. Available: https://repositorio.lneg.pt/bitstream/10400.9/1501/1/EWEA_Amsterdam_RMarujo_PCosta_MFernandes_AEstanqueiro.pdf

[29] J. Silva, F. Marques da Silva, A. Couto, and A. Estanqueiro, “A method to correct the flow distortion of offshore wind data using CFD simulation and experimental wind tunnel tests,” *J. Wind Eng. Ind. Aerodyn.*, vol. 140, 2015, doi: 10.1016/j.jweia.2015.01.017.

[30] J. M. L. M. Palma, F. A. Castro, L. F. Ribeiro, A. H. Rodrigues, and A. P. Pinto, “Linear and nonlinear models in wind resource assessment and wind turbine micro-siting in complex terrain,” *J. Wind Eng. Ind. Aerodyn.*, vol. 96, no. 12, pp. 2308–2326, 2008, doi: 10.1016/j.jweia.2008.03.012.

[31] C. G. Nunalee, C. Meißner, A. Vignaroli, N. Carolina, and R. Nc, “Downscaling MERRA mesoscale data for the generation microscale wind fields using CFD,” in *Spain: Europe’s Premier Wind Energy Event*, 2014, p. 1.

[32] C. Schmitt, C. Meissner, and D. Weir, “Influence Of Thermal Stratification on CFD Simulations,” *Europe’s Premier Wind Energy Event poster*. EWEA, Brussels, p. 1, 2011

[Online]. Available: https://windsim.com/Windsimarchive/library -- papers-presentations/Influence Of Thermal Stratification on CFD Simulations.pdf

[33] F. Castellani, D. Astolfi, M. Mana, M. Burlando, C. Meißner, and E. Piccioni, “Wind Power Forecasting techniques in complex terrain: ANN vs. ANN-CFD hybrid approach,” *J. Phys. Conf. Ser.*, vol. 753, no. 8, p. 082002, Sep. 2016, doi: 10.1088/1742-6596/753/8/082002. [Online]. Available: https://repositorio.lneg.pt/bitstream/10400.9/1501/1/EWEA_Amsterdam_RMarujo_PCosta_MFernandes_AEstanqueiro.pdf

[34] M. Lydia, S. S. Kumar, A. I. Selvakumar, and G. E. Prem Kumar, “A comprehensive review on wind turbine power curve modeling techniques,” *Renew. Sustain. Energy Rev.*, vol. 30, pp. 452–460, Feb. 2014, doi: 10.1016/j.rser.2013.10.030.

[35] E. Yun and J. Hur, “Probabilistic estimation model of power curve to enhance power output forecasting of wind generating resources,” *Energy*, vol. 223, p. 120000, May 2021, doi: 10.1016/j.energy.2021.120000.

[36] M. Yang, C. Shi, and H. Liu, “Day-ahead wind power forecasting based on the clustering of equivalent power curves,” *Energy*, vol. 218, p. 119515, Mar. 2021, doi: 10.1016/j.energy.2020.119515.

[37] R. Blaga, A. Sabadus, N. Stefu, C. Dughir, M. Paulescu, and V. Badescu, “A current perspective on the accuracy of incoming solar energy forecasting,” *Prog. Energy Combust. Sci.*, vol. 70, pp. 119–144, 2019, doi: 10.1016/j.pecs.2018.10.003.

[38] R. A. Rajagukguk and R. Kamil, “A Deep Learning Model to Forecast Solar Irradiance Using a Sky Camera,” *Appl. Sci.*, vol. 11, no. 5049, p. 15, 2021, doi: doi.org/10.3390/app11115049.

[39] S. Dev, F. M. Savoy, Y. H. Lee, and S. Winkler, “Estimating solar irradiance using sky imagers,” *Atmos. meas. Tech*, vol. 12, pp. 5417–5429, 2019, doi: https://doi.org/10.5194/amt-12-5417-2019.

[40] J. Antonanzas, N. Osorio, R. Escobar, R. Urraca, F. J. Martinez-de-pison, and F. Antonanzas-torres, “Review of photovoltaic power forecasting,” *Sol. Energy*, vol. 136, pp. 78–111, 2016, doi: 10.1016/j.solener.2016.06.069.

[41] M. N. Akhter, S. Mekhilef, H. Mokhlis, and N. Mohamed Shah, “Review on forecasting of photovoltaic power generation based on machine learning and metaheuristic techniques,” *IET Renew. Power Gener.*, vol. 13, no. 7, pp. 1009–1023, May 2019, doi: 10.1049/iet-rpg.2018.5649.

[42] I. K. Nti, M. Teimeh, O. Nyarko-Boateng, and A. F. Adekoya, “Electricity load forecasting: a systematic review,” *J. Electr. Syst. Inf. Technol.*, vol. 7, no. 1, p. 13, Dec. 2020, doi: 10.1186/s43067-020-00021-8.

[43] S. Atique, S. Noureen, V. Roy, V. Subburaj, S. Bayne, and J. Macfie, “Forecasting of total daily solar energy generation using ARIMA: A case study,” in *2019 IEEE 9th Annual Computing and Communication Workshop and Conference (CCWC)*, 2019, pp. 0114–0119, doi: 10.1109/CCWC.2019.8666481.

[44] A. M. Foley, P. G. Leahy, A. Marvuglia, and E. J. McKeogh, “Current methods and advances in forecasting of wind power generation,” *Renew. Energy*, vol. 37, no. 1, pp. 1–8, Jan. 2012, doi: 10.1016/j.renene.2011.05.033.

[45] H. Liu, C. Chen, X. Lv, X. Wu, and M. Liu, “Deterministic wind energy forecasting: A review of intelligent predictors and auxiliary methods,” *Energy Convers. Manag.*, vol. 195, no. May, pp. 328–345, 2019, doi: 10.1016/j.enconman.2019.05.020.

[46] T. Carriere and G. Kariniotakis, “An Integrated Approach for Value-Oriented Energy Forecasting and Data-Driven Decision-Making Application to Renewable Energy Trading,” *IEEE Trans. Smart Grid*, vol. 10, no. 6, pp. 6933–6944, Nov. 2019, doi: 10.1109/TSG.2019.2914379. [Online]. Available: https://ieeexplore.ieee.org/document/8706264/

[47] C. Molnar *et al.*, “General Pitfalls of Model-Agnostic Interpretation Methods for Machine

Learning Models," in *xxAI - Beyond Explainable AI*, R. Goebe, W. Wahlste, Z.-H. Zhou, and J. Siekmann, Eds. Springer, Cham., 2022, pp. 39–68 [Online]. Available: https://link.springer.com/10.1007/978-3-031-04083-2_4

[48] L. Breiman, "Random Forests," *Mach. Learn.*, vol. 45, no. 1, pp. 5–32, 2001, doi: 10.1023/A:1010933404324. [Online]. Available: https://doi.org/10.1023/A:1010933404324

[49] H. Zheng and Y. Wu, "A XGBoost Model with Weather Similarity Analysis and Feature Engineering for Short-Term Wind Power Forecasting," *Appl. Sci.*, vol. 9, no. 15, p. 3019, Jul. 2019, doi: 10.3390/app9153019. [Online]. Available: https://www.mdpi.com/2076-3417/9/15/3019

[50] Y. Cao and L. Gui, "Multi-Step wind power forecasting model Using LSTM networks, Similar Time Series and LightGBM," in *2018 5th International Conference on Systems and Informatics (ICSAI)*, 2018, pp. 192–197, doi: 10.1109/ICSAI.2018.8599498 [Online]. Available: https://ieeexplore.ieee.org/document/8599498/

[51] E. Vinagre, T. Pinto, S. Ramos, Z. Vale, and J. M. Corchado, "Electrical Energy Consumption Forecast Using Support Vector Machines," in *Proceedings - International Workshop on Database and Expert Systems Applications, DEXA*, 2017, pp. 171–175, doi: 10.1109/DEXA.2016.046.

[52] G. Dudek, "Neural networks for pattern-based short-term load forecasting: A comparative study," *Neurocomputing*, vol. 205, pp. 64–74, 2016, doi: 10.1016/j.neucom.2016.04.021.

[53] M. Q. Raza and A. Khosravi, "A review on artificial intelligence based load demand forecasting techniques for smart grid and buildings," *Renew. Sustain. Energy Rev.*, vol. 50, pp. 1352–1372, 2015, doi: 10.1016/j.rser.2015.04.065.

[54] K. Amasyali and N. M. El-gohary, "A review of data-driven building energy consumption prediction studies," *Renew. Sustain. Energy Rev.*, vol. 81, no. 2018, pp. 1192–1205, 2018, doi: 10.1016/j.rser.2017.04.095.

[55] M. Castangia, A. Aliberti, L. Bottaccioli, E. Macii, and E. Patti, "A compound of feature selection techniques to improve solar radiation forecasting," *Expert Syst. Appl.*, vol. 178, no. March, p. 114979, Sep. 2021, doi: 10.1016/j.eswa.2021.114979.

[56] H. Liu and C. Chen, "Data processing strategies in wind energy forecasting models and applications: A comprehensive review," *Appl. Energy*, vol. 249, pp. 392–408, 2019, doi: 10.1016/j.apenergy.2019.04.188.

[57] A. Couto, P. Costa, L. Rodrigues, V. V. Lopes, and A. Estanqueiro, "Impact of Weather Regimes on the Wind Power Ramp Forecast in Portugal," *IEEE Trans. Sustain. Energy*, vol. 6, no. 3, pp. 934–942, 2015, doi: 10.1109/TSTE.2014.2334062.

[58] G. Chandrashekar and F. Sahin, "A survey on feature selection methods," *Comput. Electr. Eng.*, vol. 40, no. 1, pp. 16–28, 2014, doi: 10.1016/j.compeleceng.2013.11.024.

[59] S. Salcedo-Sanz, L. Cornejo-Bueno, L. Prieto, D. Paredes, and R. García-Herrera, "Feature selection in machine learning prediction systems for renewable energy applications," *Renew. Sustain. Energy Rev.*, vol. 90, pp. 728–741, Jul. 2018, doi: 10.1016/j.rser.2018.04.008.

[60] A. Couto, P. Costa, and T. Simões, "Identification of Extreme Wind Events Using a Weather Type Classification," *Energies*, vol. 14, no. 3944, p. 16, Jul. 2021, doi: 10.3390/en14133944.

[61] H. C. Bloomfield, D. J. Brayshaw, and A. J. Charlton-Perez, "Characterizing the winter meteorological drivers of the European electricity system using targeted circulation types," *Meteorol. Appl.*, vol. 27, no. e1858, p. 18, 2019, doi: 10.1002/met.1858.

[62] A. Couto and A. Estanqueiro, "Assessment of wind and solar PV local complementarity for the hybridization of the wind power plants installed in Portugal," *J. Clean. Prod.*, vol. 319, no. 128728, p. 12, Oct. 2021, doi: 10.1016/j.jclepro.2021.128728.

[63] F. Cassola and M. Burlando, "Wind speed and wind energy forecast through Kalman filtering of Numerical Weather Prediction model output," *Appl. Energy*, vol. 99, pp. 154–166, 2012, doi: 10.1016/j.apenergy.2012.03.054.

[64] I. González-Aparicio and A. Zucker, “Impact of wind power uncertainty forecasting on the market integration of wind energy in Spain,” *Appl. Energy*, vol. 159, pp. 334–349, Dec. 2015, doi: 10.1016/j.apenergy.2015.08.104.

[65] P. Pinson, N. Siebert, and G. Kariniotakis, “Forecasting of regional wind generation by a dynamic fuzzy-neural networks based upscaling approach,” *Eur. Wind Energy Conf. Exhib. EWEC*, 2003 [Online]. Available: http://hal.archives-ouvertes.fr/hal-00530550/

[66] Z. Liu, W. Gao, and N. Carolina, “Wind Power Plant Prediction by Using Neural Networks,” in *IEEE Energy Conversion Conference and Exposition*, 2012, p. 7, doi: 10.1109/ECCE.2012.6342351.

[67] I. Okumus and A. Dinler, “Current status of wind energy forecasting and a hybrid method for hourly predictions,” *Energy Convers. Manag.*, vol. 123, pp. 362–371, 2016, doi: 10.1016/j.enconman.2016.06.053.

[68] S. Alessandrini, F. Davò, S. Sperati, M. Benini, and L. Delle Monache, “Comparison of the economic impact of different wind power forecast systems for producers,” *Adv. Sci. Res.*, vol. 11, pp. 49–53, May 2014, doi: 10.5194/asr-11-49-2014.

[69] J. Zhang, a Florita, B. Hodge, and J. Freedman, “Ramp Forecasting Performance from Improved Short-Term Wind Power Forecasting,” *ASME 2014 Int. Des. Eng. Conf. Comput. Inf. Eng. Conf.*, no. May, 2014, doi: 10.1115/DETC2014-34775.

[70] C. Junk, L. Delle Monache, S. Alessandrini, G. Cervone, and L. von Bremen, “Predictor-weighting strategies for probabilistic wind power forecasting with an analog ensemble,” *Meteorol. Zeitschrift*, vol. 24, no. 4, pp. 361–379, 2015, doi: 10.1127/metz/2015/0659.

[71] T. Jónsson, P. Pinson, H. Madsen, and H. Nielsen, “Predictive Densities for Day-Ahead Electricity Prices Using Time-Adaptive Quantile Regression,” *Energies*, vol. 7, no. 9, pp. 5523–5547, 2014, doi: 10.3390/en7095523.

[72] M. Sun, C. Feng, and J. Zhang, “Probabilistic solar power forecasting based on weather scenario generation,” *Appl. Energy*, vol. 266, p. 114823, May 2020, doi: 10.1016/j.apenergy.2020.114823.

[73] B. Li and J. Zhang, “A review on the integration of probabilistic solar forecasting in power systems,” *Sol. Energy*, vol. 210, pp. 68–86, Nov. 2020, doi: 10.1016/j.solener.2020.07.066.

[74] Z. Zhou *et al.*, “Application of probabilistic wind power forecasting in electricity markets,” *Wind Energy*, vol. 16, pp. 321–338, 2013, doi: 10.1002/we.

[75] H. Holttinen, J. J. Miettinen, A. Couto, H. Algarvio, L. Rodrigues, and A. Estanqueiro, “Wind power producers in shorter gate closure markets and balancing markets,” in *3th International Conference on the European Energy Market (EEM)*, 2016, p. 5, doi: 10.1109/EEM.2016.7521309.

[76] R. J. Bessa, C. Moreira, B. Silva, and M. Matos, “Handling renewable energy variability and uncertainty in power systems operation,” *Wiley Interdiscip. Rev. Energy Environ.*, vol. 3, no. 2, pp. 156–178, May 2014, doi: 10.1002/wene.76.

[77] R. Bessa *et al.*, “Towards Improved Understanding of the Applicability of Uncertainty Forecasts in the Electric Power Industry,” *Energies*, vol. 10, no. 9, pp. 1402–1450, 2017, doi: 10.3390/en10091402.

[78] N. J. Cutler, H. R. Outhred, I. F. MacGill, and J. D. Kepert, “Predicting and presenting plausible future scenarios of wind power production from numerical weather prediction systems: A qualitative ex ante evaluation for decision making,” *Wind Energy*, vol. 15, no. 3, pp. 473–488, 2012, doi: 10.1002/we.485.

[79] R. J. Bessa, V. Miranda, A. Botterud, J. Wang, and E. M. Constantinescu, “Time adaptive conditional kernel density estimation for wind power forecasting,” *IEEE Trans. Sustain. Energy*, vol. 3, no. 4, pp. 660–669, 2012, doi: 10.1109/TSTE.2012.2200302.

[80] P. Li, X. Guan, and J. Wu, “Aggregated wind power generation probabilistic forecasting based on particle filter,” *Energy Convers. Manag.*, vol. 96, pp. 579–587, 2015, doi: 10.1016/j.enconman.2015.03.021.

[81] L. Delle Monache, F. A. Eckel, D. L. Rife, B. Nagarajan, and K. Searight, “Probabilistic

Weather Prediction with an Analog Ensemble," *Mon. Weather Rev.*, vol. 141, no. 10, pp. 3498–3516, Oct. 2013, doi: 10.1175/MWR-D-12-00281.1.

[82] F. Davò, S. Alessandrini, S. Sperati, L. Delle Monache, D. Airoldi, and M. T. Vespucci, "Post-processing techniques and principal component analysis for regional wind power and solar irradiance forecasting," *Sol. Energy*, vol. 134, pp. 327–338, 2016, doi: 10.1016/j.solener.2016.04.049.

[83] J. R. Andrade and R. J. Bessa, "Improving Renewable Energy Forecasting With a Grid of Numerical Weather Predictions," *IEEE Trans. Sustain. Energy*, vol. 8, no. 4, pp. 1571–1580, Oct. 2017, doi: 10.1109/TSTE.2017.2694340.

[84] C. Gallego-castillo, A. Cuerva-tejero, and O. Lopez-garcia, "A review on the recent history of wind power ramp forecasting," *Renew. Sustain. Energy Rev.*, vol. 52, pp. 1148–1157, 2015, doi: 10.1016/j.rser.2015.07.154.

[85] T. Ouyang, X. Zha, and L. Qin, "A Survey of Wind Power Ramp Forecasting," *Energy Power Eng.*, vol. 05, no. 04, pp. 368–372, 2013, doi: 10.4236/epe.2013.54B071.

[86] N. Tartaglione, "Relationship between Precipitation Forecast Errors and Skill Scores of Dichotomous Forecasts," *Weather Forecast.*, vol. 25, no. 1, pp. 355–365, Feb. 2010, doi: 10.1175/2009WAF2222211.1.

[87] A. Estanqueiro and A. Couto, "Chapter 1 - New electricity markets. The challenges of variable renewable energy," in *Local Electricity Markets*, T. Pinto, Z. Vale, and S. Widergren, Eds. Academic Press, 2021, pp. 3–20.

[88] B. Bochenek *et al.*, "Day-Ahead Wind Power Forecasting in Poland Based on Numerical Weather Prediction," *Energies*, vol. 14, no. 2164, p. 18, Apr. 2021, doi: 10.3390/en14082164.

[89] SOLARGIS, "How Solargis is improving accuracy of solar power forecasts," *Best practises*, 2017. [Online]. Available: https://solargis.com/blog/best-practices/improving-accuracy-of-solar-power-forecasts

[90] C. Schimeczek *et al.*, "D4.1 - Temporal flexibility options in electricity market simulation models," *TradeRES project deliverable*. p. 58, 2021 [Online]. Available: https://traderes.eu/wp-content/uploads/2021/10/D4.1_TemporalFlexibilityOptions_H2020.pdf

[91] EPEX Spot, "Trading at EPEX SPOT 2021," *Technical brochure*. p. 8, 2021 [Online]. Available: https://www.epexspot.com/sites/default/files/download_center_files/21-03-09_Trading Brochure.pdf

[92] F. Sensfuß, M. Ragwitz, and M. Genoese, "The merit-order effect: A detailed analysis of the price effect of renewable electricity generation on spot market prices in Germany," *Energy Policy*, vol. 36, no. 8, pp. 3086–3094, Aug. 2008, doi: 10.1016/j.enpol.2008.03.035.

[93] I. Preto, A. Couto, R. Faria, H. Algarvio, T. Santos, and A. Estanqueiro, "Optimizing wind power forecasting in day-ahead markets: the best meteorological parameters for maximum energy value," in *22nd Wind and Solar Integration Workshop (WIW 2023)*, 2023, pp. 95–102, doi: 10.1049/icp.2023.2723 [Online]. Available: https://digital-library.theiet.org/content/conferences/10.1049/icp.2023.2723

[94] G. Giebel, R. Brownsword, G. Kariniotakis, M. Denhard, and C. Draxl, "The State-Of-The-Art in Short-Term Prediction of Wind Power A Literature Overview," in *Technical Report ANEMOS.plus*, 2011, p. 109 [Online]. Available: http://ecolo.org/documents/documents_in_english/wind-predict-ANEMOS.pdf

[95] A. Couto and A. Estanqueiro, "Enhancing wind power forecast accuracy using the weather research and forecasting numerical model-based features and artificial neuronal networks," *Renew. Energy*, vol. 201, pp. 1076–1085, Dec. 2022, doi: 10.1016/j.renene.2022.11.022. [Online]. Available: https://linkinghub.elsevier.com/retrieve/pii/S096014812201655X

[96] K. Lee, B. Park, J. Kim, and J. Hong, "Day-ahead wind power forecasting based on feature extraction integrating vertical layer wind characteristics in complex terrain," *Energy*, vol. 288, p. 129713, Feb. 2024, doi: 10.1016/j.energy.2023.129713. [Online]. Available:

https://linkinghub.elsevier.com/retrieve/pii/S0360544223031080

[97] N. Ellis, R. Davy, and A. Troccoli, “Predicting wind power variability events using different statistical methods driven by regional atmospheric model output,” *Wind Energy*, vol. 18, no. 9, pp. 1611–1628, Sep. 2015, doi: 10.1002/we.1779.

[98] T. T. Warner, “Quality assurance in atmospheric modeling,” *Am. Meteorol. Soc.*, vol. 92, no. 12, pp. 1601–1610, 2011, doi: 10.1175/BAMS-D-10-00054.1.

[99] N. Ellis, R. Davy, and A. Troccoli, “Predicting wind power variability events using different statistical methods driven by regional atmospheric model output,” *Wind Energy*, vol. 18, no. 9, pp. 1611–1628, Sep. 2015, doi: 10.1002/we.1779.

[100] K. Bellinguer, V. Mahler, S. Camal, and G. Kariniotakis, “Probabilistic Forecasting of Regional Wind Power Generation for the EEM20 Competition: a Physics-oriented Machine Learning Approach,” in *2020 17th International Conference on the European Energy Market (EEM)*, 2020, p. 6, doi: 10.1109/EEM49802.2020.9221960.

[101] D. Markovics and M. J. Mayer, “Comparison of machine learning methods for photovoltaic power forecasting based on numerical weather prediction,” *Renew. Sustain. Energy Rev.*, vol. 161, no. 112364, p. 17, Jun. 2022, doi: 10.1016/j.rser.2022.112364. [Online]. Available: https://linkinghub.elsevier.com/retrieve/pii/S136403212200274X

[102] M. Castangia, A. Aliberti, L. Bottaccioli, E. Macii, and E. Patti, “A compound of feature selection techniques to improve solar radiation forecasting,” *Expert Syst. Appl.*, vol. 178, p. 114979, Sep. 2021, doi: 10.1016/j.eswa.2021.114979. [Online]. Available: https://linkinghub.elsevier.com/retrieve/pii/S0957417421004206

[103] K. Wang, X. Qi, and H. Liu, “A comparison of day-ahead photovoltaic power forecasting models based on deep learning neural network,” *Appl. Energy*, vol. 251, p. 113315, Oct. 2019, doi: 10.1016/j.apenergy.2019.113315. [Online]. Available: https://linkinghub.elsevier.com/retrieve/pii/S136403212200274X

[104] B. U. Schyska, A. Couto, L. von Bremen, A. Estanqueiro, and D. Heinemann, “Weather dependent estimation of continent-wide wind power generation based on spatio-temporal clustering,” *Adv. Sci. Res.*, vol. 14, no. 2003, pp. 131–138, May 2017, doi: 10.5194/asr-14-131-2017.

[105] C. Draxl, “On the Predictability of Hub Height Winds,” *PhdThesis, DTU Wind Energy (Risø-PhDM No 84(EN))*, p. 105, 2012 [Online]. Available: https://backend.orbit.dtu.dk/ws/portalfiles/portal/10246050/Ris_PhD_84.pdf

[106] M. Ohba, S. Kadokura, and D. Nohara, “Impacts of synoptic circulation patterns on wind power ramp events in East Japan,” *Renew. Energy*, vol. 96, pp. 591–602, 2016, doi: 10.1016/j.renene.2016.05.032.

[107] G. Strbac *et al.*, “Decarbonization of Electricity Systems in Europe: Market Design Challenges,” *IEEE Power Energy Mag.*, vol. 19, no. 1, pp. 53–63, Jan. 2021, doi: 10.1109/MPE.2020.3033397.

[108] W. Wu and M. Peng, “A Data Mining Approach Combining K -Means Clustering With Bagging Neural Network for Short-Term Wind Power Forecasting,” *IEEE Internet Things J.*, vol. 4, no. 4, pp. 979–986, Aug. 2017, doi: 10.1109/JIOT.2017.2677578. [Online]. Available: http://ieeexplore.ieee.org/document/7870674/

[109] H.-H. Bock, “Clustering Methods: A History of k-Means Algorithms,” 2007, pp. 161–172 [Online]. Available: http://link.springer.com/10.1007/978-3-540-73560-1_15

[110] P. Patel, B. Sivaiah, and R. Patel, “Approaches for finding Optimal Number of Clusters using K-Means and Agglomerative Hierarchical Clustering Techniques,” in *2022 International Conference on Intelligent Controller and Computing for Smart Power (ICICCSP)*, 2022, pp. 1–6, doi: 10.1109/ICICCSP53532.2022.9862439 [Online]. Available: https://ieeexplore.ieee.org/document/9862439/

[111] I. Jebli, F.-Z. Belouadha, M. I. Kabbaj, and A. Tilioua, “Deep Learning based Models for Solar Energy Prediction,” *Adv. Sci. Technol. Eng. Syst. J.*, vol. 6, no. 1, pp. 349–355, Jan. 2021, doi: 10.25046/aj060140. [Online]. Available: https://astesj.com/v06/i01/p40/

[112] H. A. Nielsen, H. Madsen, and T. S. Nielsen, “Using quantile regression to extend an existing wind power forecasting system with probabilistic forecasts,” *Wind Energy*, vol. 9, pp. 95–108, Jan. 2006, doi: 10.1002/we.180.

[113] K. D. Orwig *et al.*, “Recent Trends in Variable Generation Forecasting and Its Value to the Power System,” *IEEE Trans. Sustain. Energy*, vol. 6, no. 3, pp. 924–933, Jul. 2015, doi: 10.1109/TSTE.2014.2366118.

[114] R. J. Murray and I. Simmonds, “A numerical scheme for tracking cyclone centres from digital data. Part I: development and operation of the scheme,” *Aust. Met. Mag.*, vol. 39, pp. 155–166, 1991 [Online]. Available: http://www.bom.gov.au/jshess/docs/1991/murray1.pdf

[115] R. J. Murray and I. Simmonds, “A numerical scheme for tracking cyclone centres from digital data. Part II:Application to January and July general circulation model simulations.,” *Aust. Met. Mag.*, vol. 39, pp. 167–180, 1991 [Online]. Available: http://www.bom.gov.au/jshess/docs/1991/murray2.pdf

[116] P. M. Della-Marta, H. Mathis, C. Frei, M. A. Liniger, J. Kleinn, and C. Appenzeller, “The return period of wind storms over Europe,” *Int. J. Climatol.*, vol. 29, no. 3, pp. 437–459, Mar. 2009, doi: 10.1002/joc.1794.

[117] D. Renggli, “Seasonal predictability of wintertime windstorm climate over the North Atlantic and Europe,” *Dissertation Freie Universität Berlin*. p. 151, 2011 [Online]. Available: https://refubium.fu-berlin.de/handle/fub188/901

[118] E. Flaounas, V. Kotroni, K. Lagouvardos, and I. Flaounas, “Tracking winter extra-tropical cyclones based on their relative vorticity evolution and sensitivity to prior data filtering (cycloTRACK v1.0),” *Geosci. Model Dev. Discuss.*, vol. 7, no. 1, pp. 1245–1276, 2014, doi: 10.5194/gmdd-7-1245-2014.

[119] N. Helistö, J. Kiviluoma, L. Simila, K. Nienhaus, and R. Hernandez-Serna, “D2.1 - A database of TradeRES scenarios & Scenario Data,” *TradeRES project deliverable*. p. 8, 2020 [Online]. Available: https://traderes.eu/wp-content/uploads/2021/04/D2.1_TradeRES_DatabaseScenario_H2020-1.pdf

[120] F. Yang, “Comparison of Forecast Skills between NCEP GFS Four Cycles and on the Value of 06Z and 18Z Cycles,” in *27th Conference On Weather Analysis And Forecasting/23rd Conference On Numerical Weather Prediction*, 2015, p. 31.